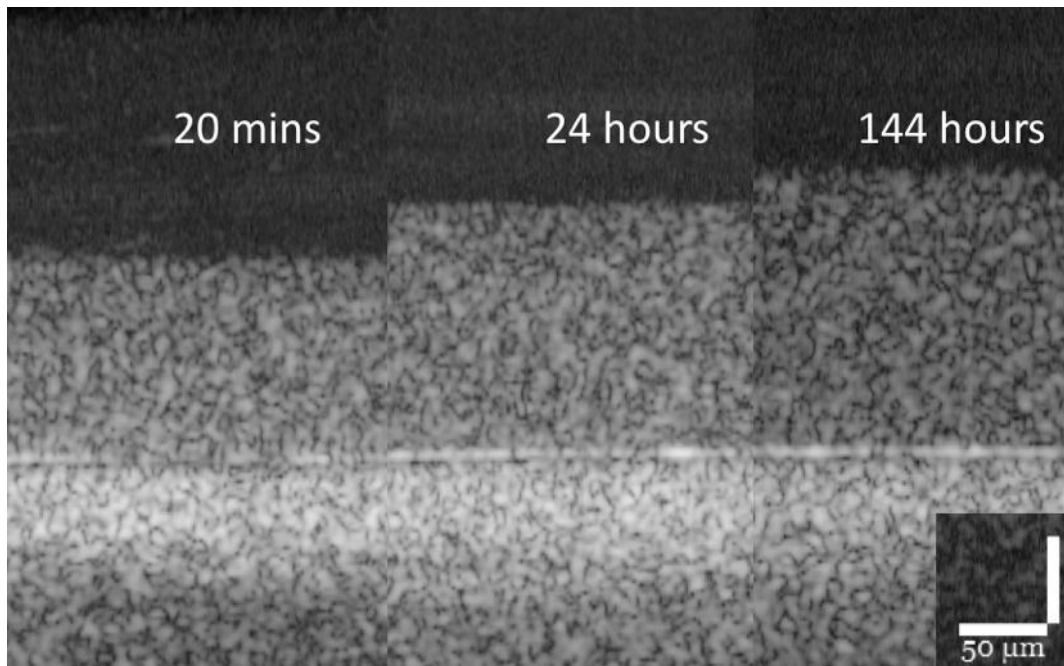


Biofilm models made from alginate-like exopolymers

Research report



Author: Yifei Gu

Course: Graduation thesis

Education/group: Water Management

Study year/semester: 2017-2018, semester 2

School: HZ University of Applied Sciences

In-company Supervisor: Natascha Pfaff

In-school 1st examiner: Emma McAteer

In-school 2nd Examiner: Mireille Martens

Wetsus, Leeuwarden, 10 June 2018

Version: 3.5

Biofilm models made from alginate-like exopolymers

Wetsus, Leeuwarden

10 June 2018

Student number: 68737

Study year: 2017-2018

Semester: 2

Report type: Research report

In-company Supervisor: Natascha Pfaff

In-school 1st examiner: Emma McAteer

In-school 2nd Examiner: Mireille Martens

Version: 3.5

Abstract

It is widely understood that biofouling is an obstacle to water treatment processes, therefore, tailored cleaning strategies are needed to increase removal efficiency. This research inquired into the swelling behaviour at the equilibrium states of target biofilm models made from alginate-like exopolymers (ALE) in laboratory condition. At this moment the density of biofilm was introduced to profile its binding strength. At ALE biofilm model's equilibrium state, the density will be illustrated by its swelling height over time, the amount of organic and inorganic materials within the biofilm model, and the cake-layer resistance. This research observed and suggested that 3mM calcium ion concentration within feed solution is the threshold to control ALE biofilm models' density.

Table of Contents

Abstract

Abbreviation list

1. Introduction	1
Problem statement	1
Research objectives	2
Research questions	2
Boundary conditions	3
Report outline	3
2. Theoretical framework	4
A brief insight to biofilms' structure	4
The background of EPS.....	5
The basics of biofilm models.....	5
The cake-layer resistance of ALE biofilm models	6
The approach to understand ALE.....	6
Membrane cleaning strategies	7
3. Method	8
ALE extraction from EPS of aerobic granular sludge	8
ALE biofilm (models) series generation	9
Continuous monitoring of swelling behaviour of ALE biofilm (models)	11
Data processing and analysing	11
Cake-layer resistance.....	12
TSS/VSS test	12
IC/ICP-OES test	13
4. Results.....	14
The interpretation of different equilibrium states.....	14
The influence of feed solution on ALE biofilms dry mass compositions	14
The effect of the ion concentration within the biofilm on its swelling behaviour.....	16
Experiment series one.....	17
Experiment series two.....	18
Experiment series three.....	19
The variation of cake-layer resistance	20
5. Discussion	23
General reflection: potential influence of microorganism.....	23
A structural hamper: the effect of transmembrane pressure	24
Other stochastic disturbances	24

6. Conclusion & recommendation.....	25
Answers to the research questions.....	25
Recommendations for future experiments	26
Recommendations for tailored cleaning strategies	26
Bibliography	27
Appendix 1: Functions of EPS in bacterial biofilms	30
Appendix 2: Detailed experiment protocols	31
Appendix 3: TSS/VSS percentage plots R coding	33

Figure 1 Mechanisms of membrane fouling in membrane bioreactors; EPS stands for extracellular polymeric substances, SMP stands for soluble microbial products (Iorhemen, Hamza, & Tay, 2016).....	1
Figure 2 Stages of biofilm development (Lyme, 2015)	4
Figure 3 Alginate chain (Williams, 2007)	6
Figure 4 The ‘egg-box’ model depicting alginate junction zone formation (Williams, 2007)	7
Figure 5 Experimental pathway	8
Figure 6 Acidic form gel-like ALE pellet after centrifugation	8
Figure 7 Dead-end filtration system	9
Figure 8 Dead-end filtration system illustration, producing 2 films under the same condition	9
Figure 9 Produced ALE biofilm models 20 minutes after dead-end filtration stored in Petri dish.....	10
Figure 10 Optical coherence tomography (OCT) device.....	11
Figure 11 Example relationship among sludge sample, TSS, and VSS	13
Figure 12 Net calcium ions within ALE biofilm models experiment series 1	15
Figure 13 Net calcium ions within ALE biofilm models experiment series 2	15
Figure 14 Net calcium ions within ALE biofilm models experiment series 3	16
Figure 15 Swelling behaviour and VSS density overtime experiment series one	17
Figure 16 Swelling behaviour and VSS density overtime experiment series two	18
Figure 17 Swelling behaviour and VSS density overtime experiment series three	19
Figure 18 ALE biofilm models with only 6mM KCl in feed solutions. From left to right: 2 minutes after being taken out of Amicon cell; 20 minutes out of Amicon cell; 24 hours out of Amicon cell and be transported for the test.....	21
Figure 19 Normalised cake-layer resistance against VSS mass for each experiment series	22
Figure 20 Internal porosity of one sample in experiment series 3, 3mM CaCl ₂ •2H ₂ O & 6mM KCl after 144hours.....	23

Table 1 ALE biofilm models generation series	10
Table 2 Swelling phases of ALE biofilm models.....	14
Table 3 Time to reach the equilibrium state and Cake-layer resistance under different feed solutions	20

Abbreviation list

ALE: alginate-like exopolymers

EPS: extracellular polymeric substances

IC: ion chromatography

ICP-OES: inductive coupled plasma optical emission spectrometry

J : permeate flux

OCT: optical coherence tomography

R_{cl} : cake-layer resistance

$R_{membrane}$: membrane intrinsic resistance

R_{total} : total biofilm resistance

TMP: transmembrane pressure

TSS: total suspended solids

VSS: volatile suspended solids

WWTP: wastewater treatment plant

η : water viscosity at a given temperature

1. Introduction

Problem statement

Biofouling in wastewater treatment plant (WWTP) membrane filtration processes is the accumulation of undesired microorganisms, caused by sessile microbial communities adhering to membrane surfaces (Garrett, Bhakoo, & Zhang, 2008). It reduces their filtration efficiency because it blocks the membranes over time (see Figure 1). To ensure the function of membranes, regular cleaning is necessary (Nguyen, Roddick, & Fan, 2012). The cleaning process, however, is tricky and the biofouling is hard to remove due to the resistance of extracellular polymeric substances (EPS) matrixes (Arnal, García-Fayos, & Sancho, 2011; Garrett, Bhakoo, & Zhang, 2008). The EPS are excreted from the adhering bacteria to stabilise the biofouling structures under hostile conditions, which further contributes to the problems such as clogging of equipment, energy losses, and health risk etc. (Bogino, Oliva, Sorroche, & Giordano, 2013; Gerritse & Huurne, 2011; van der Borden, van der Werf, van der Mei, & Busscher, 2004).

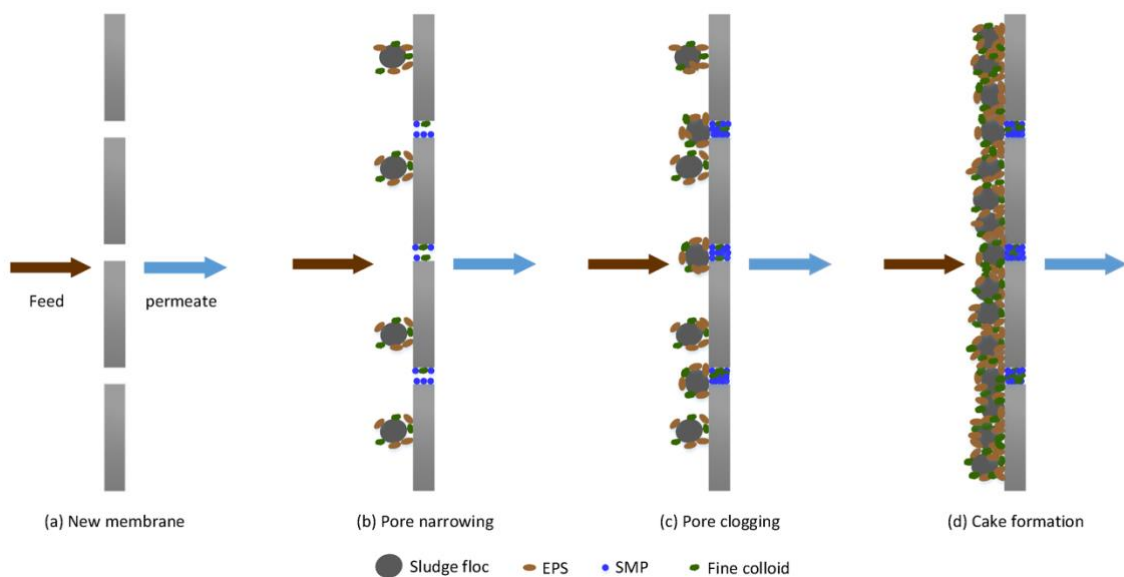


Figure 1 Mechanisms of membrane fouling in membrane bioreactors; EPS stands for extracellular polymeric substances, SMP stands for soluble microbial products (Iorhemen, Hamza, & Tay, 2016)

As a thin layer of biofouling, the biofilm is ideal to study proper cleaning strategies. Since EPS within biofilms provided the structural integrity, the physiochemical bonds and how they determine the strength of biofilms need to be investigated (Nguyen, Roddick, & Fan, 2012). According to existing research, various factors can influence the strength of biofilms; such are for example the biofilm composition, the kind of membranes or biocide application. These influences can often not be adequately controlled and thus can hamper the biofilm studies (Strathmann, Griebel, & Flemming, 2000). Therefore, biofilms in laboratory condition are necessary in this project to control variables.

Focusing on the composition, it was found that the EPS of several biofilms contain alginate-like exopolymers (ALE) (Lin, de Kreuk, van Loosdrecht, & Adin, 2010). Similar to alginate biofilms, ALE biofilms also have gel formation property with the existence of calcium ions (Lin, de Kreuk, van Loosdrecht, & Adin, 2010). On the other hand, these ALE films keep swelling at least to 10 days after production, while films made from commercially available alginate usually reaches an equilibrium state after 24h (Davidovich-Pinhas & Bianco-Peled, 2009). In this context, the calcium-based ALE biofilm models will be further studied to understand their swelling behaviours with a focus on the changing ionic strength and the presence of monovalent potassium ions.

Research objectives

There are three objectives for this project. First, analysing the dry mass compositions within ALE films at their equilibrium states. The expectation is that the different dry mass compositions of the biofilms can lead to different equilibrium water contents because the equilibrium depends on the molecular interactions among the dry mass composition of the films and salts in feed solution (Melo, Bott, Fletcher, & Capdeville, 1992). The other part is monitoring the swelling behaviour of the ALE biofilm models at different feed solution concentrations over time until they reach the equilibrium. This can be broken down to the influence of ionic strength and calcium and potassium ions concentration under certain time period and pressure state. By comparing different compositions and identifying the vital components that contribute to biofilms' strength, weak points of biofilms can be identified. Based on that, suggestions can be made to develop tailored cleaning strategies.

Research questions

On behalf of the objectives, the following main and sub research questions are identified:

How does the ionic composition within the surrounding solution influence the density of an ALE biofilm model?

Since the structural integrity namely the strength is difficult to thoroughly study, at this moment the density of biofilm is introduced to profile the binding strength. At ALE biofilm model's equilibrium state, the density will be illustrated by the swelling height of the biofilm model over time, the amount of organic and inorganic material within the biofilm model, and the cake-layer resistance.

What are the equilibrium states for the ALE biofilm models under different feed solutions?

How does different ionic composition within the feed solution affect the organic and inorganic content within an ALE biofilm model?

What effect has the ion composition within an ALE biofilm model on its swelling behaviour?

How does the cake-layer resistance vary along with the changing biofilm feed solutions?

Boundary conditions

To further investigate the gel properties of the ALE biofilm models, a parallel measurement of the viscoelastic properties will be generated adjacent to this project to quantify the effect of water content. This experiment will be carried out by another student in Wetsus to research the failure point of the formed gel. Furthermore, the molecular interactions within the real biofilms are too complicated to illustrate for now. Therefore, this project will only look into the swelling behaviour of biofilm models based on ALE models. In addition, the equilibrium state in this project is indicated by the relatively maximum swelling height. According to pre-observation, the ALE biofilm models will swell to certain maximum height, but then they can collapse/shrink after a longer time, which can be partially due to the biofilm dispersal process or their inner molecular interactions (Kaplan, 2010). However, both of these cases are out of the scope of this project.

Report outline

Chapter 2 presents the theoretical framework that is followed in this study. It describes the research background and explains the terms and conditions during this project. The next chapter gives the experimental protocol and the guideline for data analysis of this study. Chapter 4 discusses the results and implications of this study, followed by the discussion in chapter 5 and the conclusion & recommendation in chapter 6.

2. Theoretical framework

This chapter contains two main goals; the first one is to introduce the physiochemical properties of the source materials where ALE is extracted from since specific extraction protocols represent their special identities. The other one is the literature study of gel formation process and swelling behaviour on the ALE biofilms. It also contains a brief review of current membrane cleaning strategies.

A brief insight into biofilms' structure

Generally speaking, the biofilm is composed of the aggregated microbial at a solid-liquid interface that encased in the highly hydrated extracellular polymeric substances (EPS) matrix (Nguyen, Roddick, & Fan, 2012). The structured microbial communities play an important role in forming biofilms. The sequence of biofilm formation includes: 1) the adsorption of organic species and suspended particles on the wetted membrane surface to form a prototype film; 2) the transport of the microbial cells to the prototype; 3) the attachment of the microbial cells to the membrane surface; 4) the growth and metabolism of the attached microorganisms and mature biofilm development; 5) the limitation of biofilm growth by fluid shear forces to achieve a steady state fouling resistance and the disperse of free floating biofilm particles; 6) the iterative process (Al-Ahmad, Aleem, Mutiri, & A. Ubaisy, 2000; Stoodley, Sauer, Davies, & Costerton, 2002).

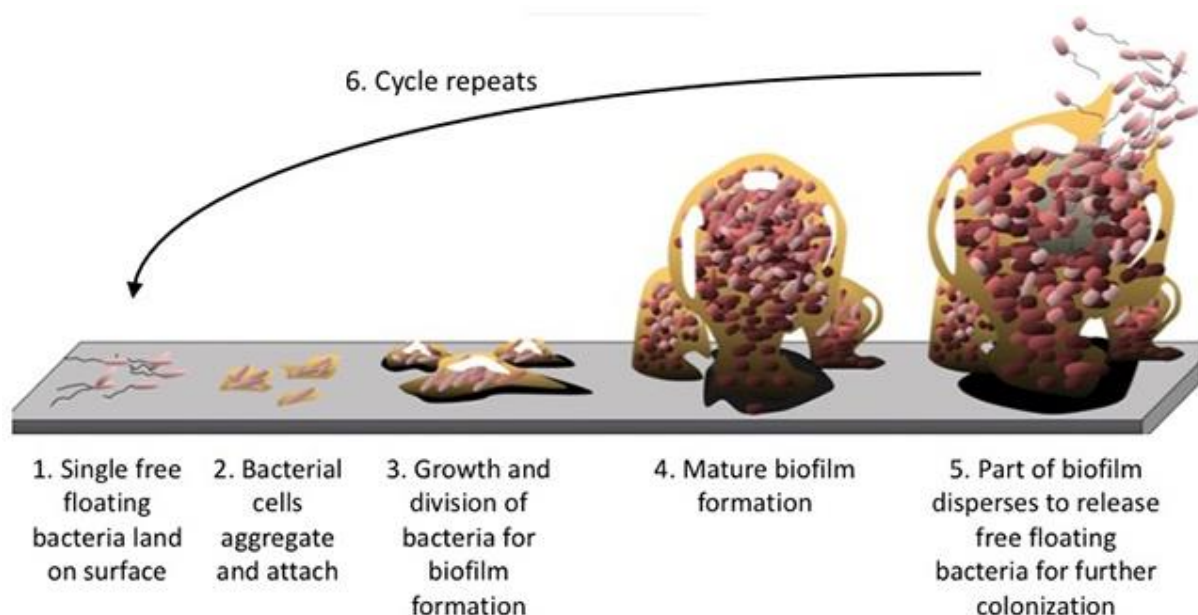


Figure 2 Stages of biofilm development (Lyme, 2015)

However, in most biofilms, the occurrence of microorganisms is less than 10% of their dry mass, whereas the majority compensation of biofilms is the EPS matrix, which accounts more than 90% (Flemming & Wingender, 2010). During the biofilm formation processes, EPSs

are generally required not for initial adhesion but later architectural development of its matrix (Wingender, Neu, & Flemming, 1999). Morphologically, biofilms are often permeated by channels that act as a circulatory system, allowing the bacteria to apply metabolic activities with outside circumstances (Bogino, Oliva, Sorroche, & Giordano, 2013). In other words, the production and quantity of EPS excreted from structured microbial communities are vital to their formation and maintenance (Flemming & Wingender, 2010).

The background of EPS

EPS have been shown to be a rich matrix of polymers; polysaccharides and proteins are the major components of EPS. Other components, such as humic acids, nucleic acids, lipids, uronic acids have also been shown to appear in a certain amount in EPS (Lin, et al., 2014; McSwain, Irvine, Hausner, & Wilderer, 2005). The functions of EPS are well studied and presented in Appendix 1. The main mechanism of EPS is to facilitate the formation of a gel-like matrix that keeps bacteria together in biofilms, contribute to the adherence of bacteria, and protect them against harsh environmental conditions (McSwain, Irvine, Hausner, & Wilderer, 2005; Wingender, Neu, & Flemming, 1999).

As the essential component in biofilm, EPS compositions can vary greatly among biofilms, depending on the microorganisms' present, the shear forces experienced, the temperature and the availability of nutrients. These parameters are usually hard to control, which makes it difficult to specify the influence of various factors (Flemming & Wingender, 2010; Strathmann, Griebe, & Flemming, 2000). However, the identification of EPS components is also complicated as well as the efficiency of EPS components isolation (Wingender, Neu, & Flemming, 1999). EPS from environmental biofilms can contain an immense range of components that each requires different extraction method. In a mixed-species biofilm, different microbial communities contribute to their own and often specific EPS structures and then merge into a more complex mixture. Moreover, these excreted EPS can remain in the biofilm matrix even after their producers have died or left the biofilm (Flemming & Wingender, 2010). Therefore, the approach of using biofilm model was applied in this project to control the compositions and to determine the reactants.

The basics of biofilm models

To control the variables, the base material of generated biofilms is strictly controlled. NADIR UP150 ultrafiltration membrane will be used in this project. As a professional product, this kind of membrane is widely used in a concentration of large organic solutes in both water and process applications and can be used for membrane bioreactor. The permanently hydrophilic and chemically resistant abilities ensure its performance and stability in generating biofilms (Microdyn NADIR, 2018). On the other hand, as the microbial feed to this typical membrane, alginate-like exopolymers (ALE) extracted from EPS will be used to produce cake-layer on the membrane surface, which will be further investigated in its swelling behaviour under different dry mass compositions.

To strictly control the variables, aerobic granular sludge from wastewater treatment plant (WWTP) in Garmerwolde is used as the source extraction material. This WWTP in Garmerwolde is the second Dutch Nereda plant. As an innovative technology, this Nereda system is entirely based on biology reactions. With little dependence on chemicals, the WWTP provides the eco-friendly and efficient solution for municipal wastewater. Furthermore, the generated aerobic granular sludge in this system has unique settling properties (Dutch Water Sector, 2013; Royal HaskoningDHV, 2013).

The cake-layer resistance of ALE biofilm models

The alginate-like exopolymers can interact with the membrane surface by forming a cake layer in colloidal form (Nguyen, Roddick, & Fan, 2012). According to Derlon, et al. (2016), biofilm composition and pressure condition can affect the biofilm hydraulic resistance. The total resistance of produced ALE biofilm models is composed of the intrinsic resistance of the membrane and the cake-layer resistance (Derlon, et al., 2016; Desmond, Best, Morgenroth, & Derlon, 2018). As mentioned, the biofilm composition in this project is controlled. Therefore, the pressure changing plays an important role in define the cake-layer resistance. As a highly compressible structure, transmembrane pressure (TMP) imposed on the cake layer can influence its resistance (Charfi, Harmand, Amar, Grasmick, & Heran, 2014; Derlon, et al., 2016). At the same time, the instantaneous pressure changes also impact the cake-layer resistance, namely the compression/relaxation of the biofilm models when they are taken out of the dead-end filtration system (Derlon, et al., 2016). To mitigate the effect of instantaneous pressure change, cake-layer resistance will be calculated when it is inside the dead-end filtration system.

The approach to understanding ALE

According to Lin, et al. (2010), alginate-like exopolymers (ALE) is one of the major exopolymers in aerobic granules. The properties of ALE are similar to those commercial alginates extracted from brown algae. Therefore, the structural model of alginate is used as the reference in this research. It takes 24 hours for commercially available alginate biofilms to reach its equilibrium and its swelling kinetics drops around 2 hours after production (Davidovich-Pinhas & Bianco-Peled, 2009).

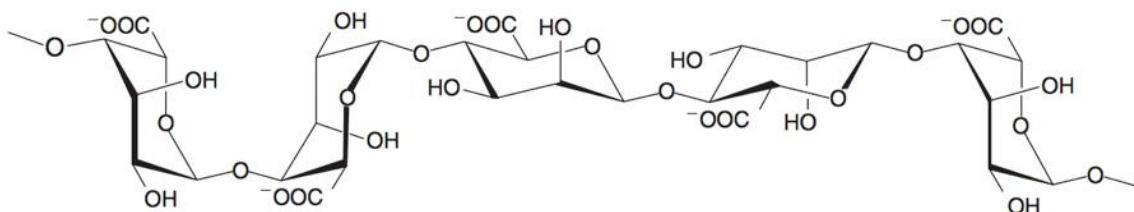


Figure 3 Alginate chain (Williams, 2007)

ALE was shown to be soluble under relatively mild alkaline conditions, but it can form gels under acidic pH (pH lower than 4.5) and in the presence of divalent cations, especially with the existence of Ca^{2+} (Lin, de Kreuk, van Loosdrecht, & Adin, 2010; Seviour, Yuan, van Loosdrecht, & Lin, 2012), which can be used in the centrifugation process during extraction and the identification after extraction. As mentioned before, aerobic granular sludge from municipal WWTP is the source material for ALE extraction. The extractable ALE is approximately 15-25% of the organic fraction in aerobic granular sludge (Pronk, Neu, Loosdrecht, & Lin, 2017) and the yield of extractable ALE was reached 160 ± 4 mg/g (VSS ratio) (Lin, de Kreuk, van Loosdrecht, & Adin, 2010).

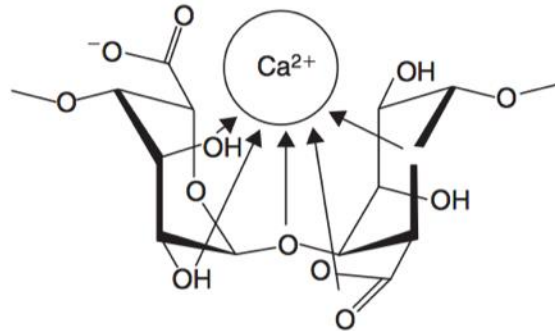


Figure 4 The 'egg-box' model depicting alginate junction zone formation (Williams, 2007)

Membrane cleaning strategies

Membrane cleaning is necessary to increase the filtration efficiency by weakening the fouling layer attachment. Cleaning strategies nowadays can be divided into physical and chemical cleaning. Unlike chemical cleaning, physical cleaning is the most common technique and has less side effect on membrane life. Regarding physical cleaning, backwashing is widely used in industrial scale, whereas other techniques like ultrasound, electrical fields etc. are still foreseen development (Nguyen, Roddick, & Fan, 2012).

3. Method

There are four main aspects of this chapter, first is the ALE extraction procedures. Regarding the complexity of EPS, specific protocols are necessary for extraction. The second one is the guideline for producing ALE biofilm (models). The third one is the continuous monitoring of the swelling behaviour of ALE biofilm models. The last one is the procedure and analytic method in data processing and analysing. The detailed protocols are presented in the appendix. The following figure illustrates the practical pathway.

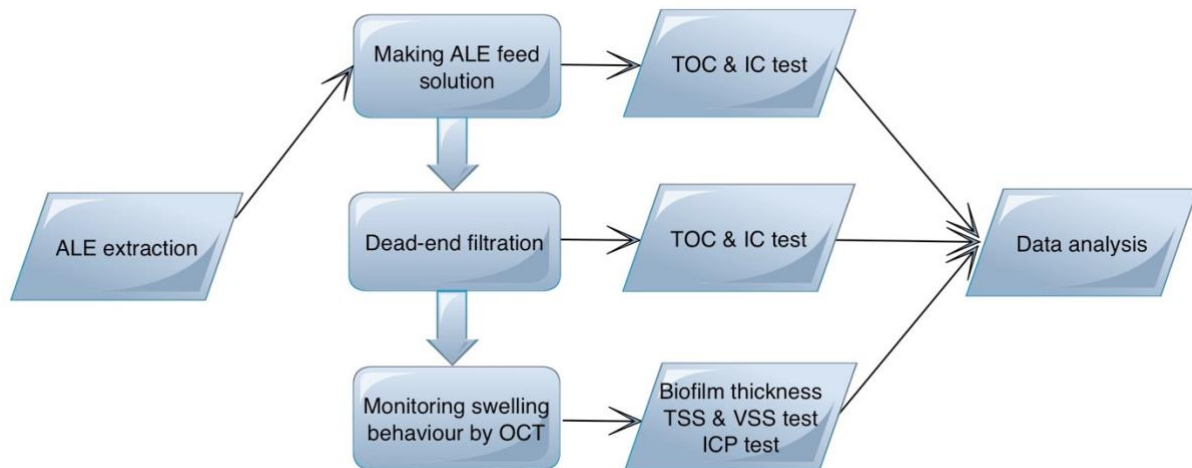


Figure 5 Experimental pathway

ALE extraction from EPS of aerobic granular sludge

According to Seviour, et. al (2012), a high pH extraction in combination with ultrasound treatment gave the highest EPS yield among several examined physical and chemical extraction methods. It is also expected a denaturation process of EPS molecules under high temperature (80°C). Therefore, the combination of high pH and water bath can ensure higher EPS yield (D'Abzac, Bordas, Van Hullebusch, Lens, & Guibaud, 2010).

It is noteworthy that ALE formed gels under acidic condition (pH lower than 4.5) and in the presence of calcium ion (Seviour, Yuan, van Loosdrecht, & Lin, 2012). The adjacent figure shows the extracted ALE pellet. Extra ALE samples were stored in -80°C condition to minimize the influence of microorganisms.



Figure 6 Acidic form gel-like ALE pellet after centrifugation

According to the ionic hydrogel formation properties of ALE, if drop-shaped (spherical) beads formed after dripping the extract into calcium chloride (CaCl₂) solution, the extract EPS is proved as ALE. Otherwise, it will disperse in the CaCl₂ solution (Felz, Al-Zuhairy, Aarstad, Loosdrecht, & Lin, 2016).

ALE biofilm (models) series generation

This is the core experimental part of this project. ALE biofilm models were produced through the dead-end filtration setups (see Figure 7&8). Through each filtration setup, approximately 600 grams feed solution was filtered and each dead-end filtration course produced two biofilm models. Every dead-end filtration course was conducted in duplicates for each combination of feed solution. In this way, 4 biofilm models will be produced for the same concentration of feed solution.



Figure 7 Dead-end filtration system

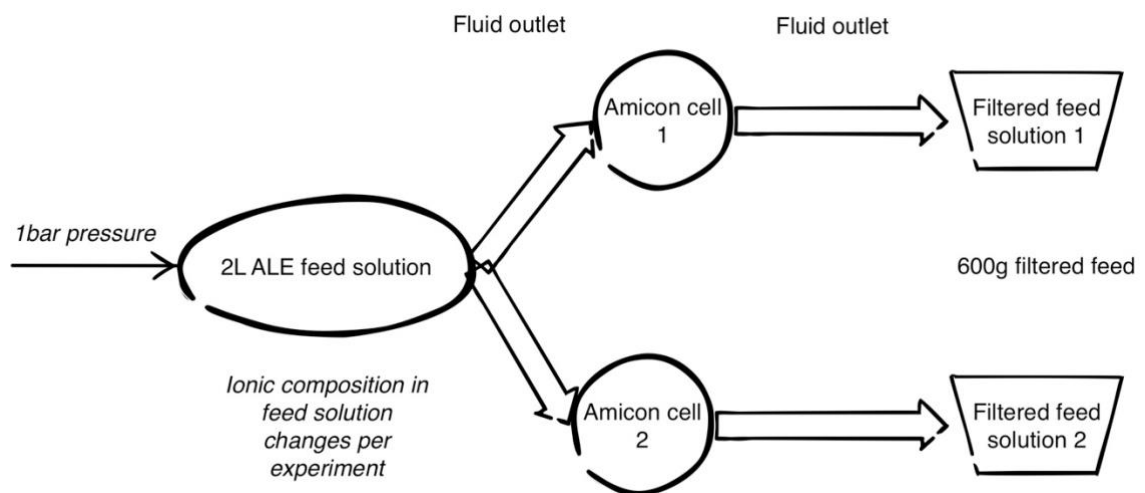


Figure 8 Dead-end filtration system illustration, producing 2 films under the same condition

In each feed solution, the ALE concentration is controlled at 120mg/L. Since there is no other ion input, the ionic composition within the ALE biofilm models changes with the variant of feed solutions. The produced ALE biofilm models will be stored in Petri dishes with the storage solution that has same ion composition as feed solutions to minimize the ion exchange within the films during monitoring phase. The following table indicates the different combinations of feed solutions and ionic strengths. In this context, ALE biofilm models with different ion concentration and ionic strength will be produced accordingly.



Figure 9 Produced ALE biofilm models 20 minutes after dead-end filtration stored in Petri dish

Table 1 ALE biofilm models generation series

Experiment1 keep ionic strength at 24mM		
	CaCl ₂ /mM	KCl/mM
Combination1	0	24
Combination2	3	15
Combination3	6	6
Combination4	8	0
Experiment2 keep CaCl ₂ at 6mM		
	KCl/mM	IS/mM
Combination1	24	42
Combination2	15	33
Combination3	6	24
Combination4	0	18
Experiment3 keep KCl at 6mM		
	CaCl ₂ /mM	IS/mM
Combination1	0	6
Combination2	3	15
Combination3	6	24
Combination4	8	30
Combination5	12	42

Continuous monitoring of swelling behaviour of ALE biofilm (models)

The main aim of this process is to compare the swelling rate of films that were produced and stored under different ion conditions. The equilibrium state of the ALE biofilm models at different water compositions was determined by monitoring their swelling behaviour over time using the optical coherence tomography (OCT) device below. OCT can provide the overall thickness, internal porosity and surface topology of monitored samples in resolution $\pm 10 \mu\text{m}$ (Desmond, Best, Morgenroth, & Derlon, 2018). Following the protocols in the appendix, the swelling height of the ALE biofilm models within certain time intervals was determined. Combining with the later determination of dry mass/VSS, density chart of the biofilm models was plotted. In this context, how fast the different films swell and how much they in the end 'grow' in relation to their original size, namely the relative increase was analyzed.

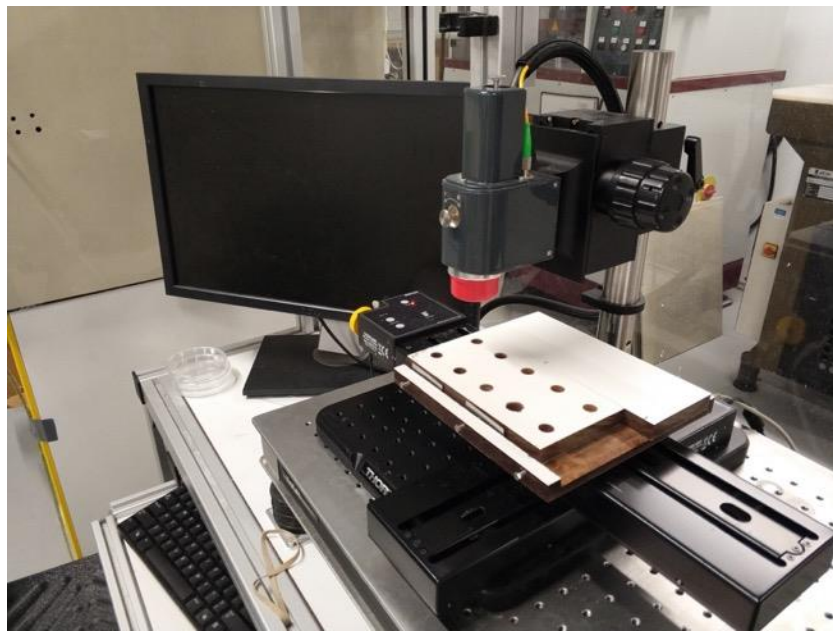


Figure 10 Optical coherence tomography (OCT) device

Data processing and analysing

The aim of this process is analysing the water contents of feed solution and the dry mass compositions within ALE biofilms at their equilibrium states. It is expected that different dry mass compositions within the biofilms can lead to different density and the compositions are dependent on the changing ionic composition within feed solutions. To examine that, total suspended solids (TSS) and volatile suspended solids (VSS) tests are necessary to determine the number of dry mass compositions within the biofilm models. As for the ion concentration within feed solutions, ion chromatograph (IC) test for the feed solution and further inductive coupled plasma optical emission spectrometry (ICP-OES) tests for ash is needed. The combination of the density with cake-layer resistance data can give insight into the structure in the films.

Cake-layer resistance

The cake-layer resistance was calculated directly after the dead-end filtration. Permeated flux through the membrane and the cake-layer resistance is strongly related (Dreszer, et al., 2013).

$$J = \frac{\Delta V}{A \cdot \Delta t} [L m^{-2} h^{-1}] \quad (1)$$

The permeate flux J through a membrane in equation 1 (Desmond, Best, Morgenroth, & Derlon, 2018; Dreszer, et al., 2013) is expressed as the changing amount of solution flowing through a certain membrane area (0.003848m²) in a certain time. To receive a steady value, the data from the last hour of dead-end filtration is used.

$$R_{total} = \frac{TMP}{\eta \cdot J} [m^{-1}] \quad (2)$$

As mentioned before, transmembrane pressure (TMP) imposed on the biofilm can influence its resistance. The η in equation 2 (Desmond, Best, Morgenroth, & Derlon, 2018; Dreszer, et al., 2013) represents the dynamic viscosity of water at a given temperature. In this condition, the $\eta = 0.497 \cdot (42.5 + T \text{ (in } ^\circ\text{C)})^{-1.5}$ while the temperature in the lab is controlled at 22 °C. R_{total} is the total resistance of biofilm.

$$R_{cl} = R_{total} - R_{membrane} [m^{-1}] \quad (3)$$

The cake-layer resistance in equation 3 (Desmond, Best, Morgenroth, & Derlon, 2018; Dreszer, et al., 2013) is the measured total biofilm resistance minus the intrinsic resistance of the NADIR UP150 ultrafiltration membrane ($R_{membrane}$). The equation 1 will be used again to calculate $R_{membrane}$ 10 minutes before the end of clean water flux by demineralised water.

TSS/VSS test

TSS/VSS test is widely used for assessing sludge solids. In this project, it was applied to the ALE cake layers, which were scratched from the membrane after monitoring the swelling behaviour. The common method is as follows: samples will be dried at 105 °C for 24 hours to determine the dry matter and then burnt at 550 °C for 2 hours to obtain mineral matter in ash form. In this process, VSS can represent the organic materials and the remains are the inorganic matters (Salsabil, Laurent, Casellas, & Dagot, 2010). The following graph indicates the relationship among sludge sample, TSS, and VSS.

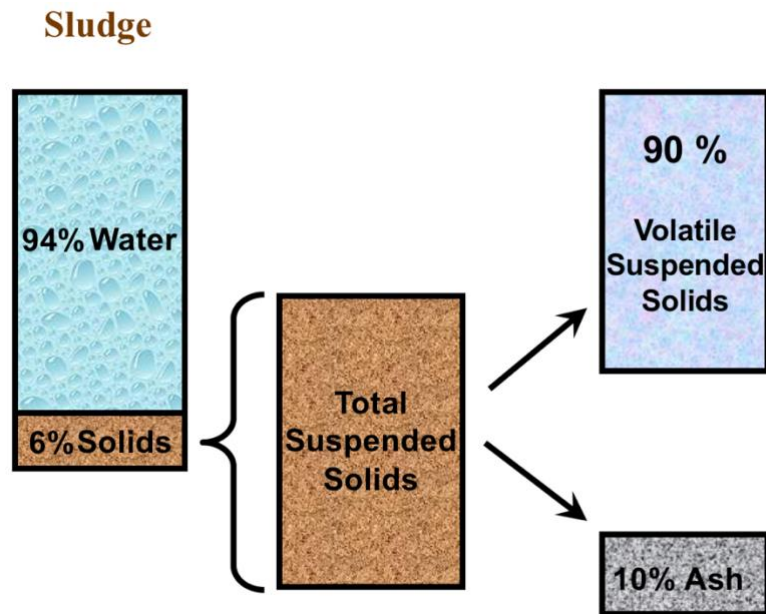


Figure 11 Example relationship among sludge sample, TSS, and VSS

For each feed solution combination, the TSS/VSS value is the average of quadruplet samples. After 2 hours of exposure into 550 °C, the organic part of the samples (namely VSS) were burnt. The remaining ash was used for microwave digestion in 69% HNO₃ and ICP-OES to further analyse the content of calcium, potassium, sodium, iron, sulphur, and boron, whereas the first three ones are scientifically of interested, the rest ones are analysed for their appearance.

IC/ICP-OES test

Ion chromatography (IC) test is a widely used standard method to determine the inorganic anions in water which has low detection limits. IC affords multiple detections in a single sample run. It is also capable for quantitative cation analysis (Sinniah & Piers, 2001; Wartena, 2010). Inductive coupled plasma optical emission spectrometry (ICP-OES) has a wide range elemental application area. By detecting the spontaneous emission of photons from excited atoms, ICP-OES is capable of producing less noisy but efficient and reproducible element determination. It is also applicable to handle acidic samples while IC test cannot (Hou & Jones, 2000; Kersaan-Haan & Heegstra, 2010).

Considering the mechanism of IC test, the ash content is hard to dissolve in water. Therefore, microwave digestion with 69% HNO₃ was applied to treat the ash content and later on the ICP-OES test. Due to the porosity, it is inevitable to have certain remained storage solution in films. To obtain a precise value, the ion amount added by the storage solution will be deducted. In this context, the water content in TSS/VSS test will be used to calculate how much ions the storage solution adds.

4. Results

With the aid of tables and figures, this chapter will illustrate the experimental results from these four perspectives, namely 1) the equilibrium states in ALE biofilms swelling behaviours; 2) the influence of feed solution to ALE biofilms dry mass compositions; 3) the effect of the ion composition within the biofilm on its swelling behaviour; and 4) the variation of cake-layer resistance. Conclusions can be drawn accordingly.

The interpretation of different equilibrium states

Predetermined as the boundary condition, the equilibrium state in this project is indicated by the relatively maximum swelling height which is measured by the optical coherence tomography (OCT) device. According to observation, the ALE biofilm models in trial experiments can swell to certain maximum height but they can then collapse in the long term. A lot of reasons can cause this phenomenon, like the biofilm dispersal process or their inner molecular interactions (Kaplan, 2010) etc. The ALE biofilm models monitored by OCT had been through the following phases in the following table.

Table 2 Swelling phases of ALE biofilm models

Swelling phases	Description
Initial phase	Biofilm models monitored directly after production, usually around 20 mins and 2 hours in comparison to alginate biofilms
Steady swelling phase	Biofilm models monitored after certain days when cake-layer is smooth
Equilibrium state	The time when the ALE biofilm models reach its maximum steady swelling height, usually 10 days after production

According to existing research, the swelling kinetics of alginate biofilms, as a reference object, drops 2 hours after production whereas the ALE biofilm models can continue swell for more than 10 days (240 hours) (Davidovich-Pinhas & Bianco-Peled, 2009). However, the time to reach equilibrium state changes for ALE biofilm models produced in different series. Due to timing reason, the observation for swelling behaviour usually ends around 12 days (288 hours) after production.

The influence of feed solution on ALE biofilms dry mass compositions

As mentioned in above chapters, the base membrane materials and the source sludge materials are strictly controlled to generate these ALE biofilm models. Therefore, the dry mass compositions within these ALE biofilms models depend on the changing ion concentrations of the feed solutions. There is an exception for the samples with only KCl in the feed solution. They are fragile and easy to detach from the base membrane. Therefore, it is inevitable to transfer too many ions in feed solution into the biofilm models' system when conduct TSS/VSS test. In this case, these samples will not be included.

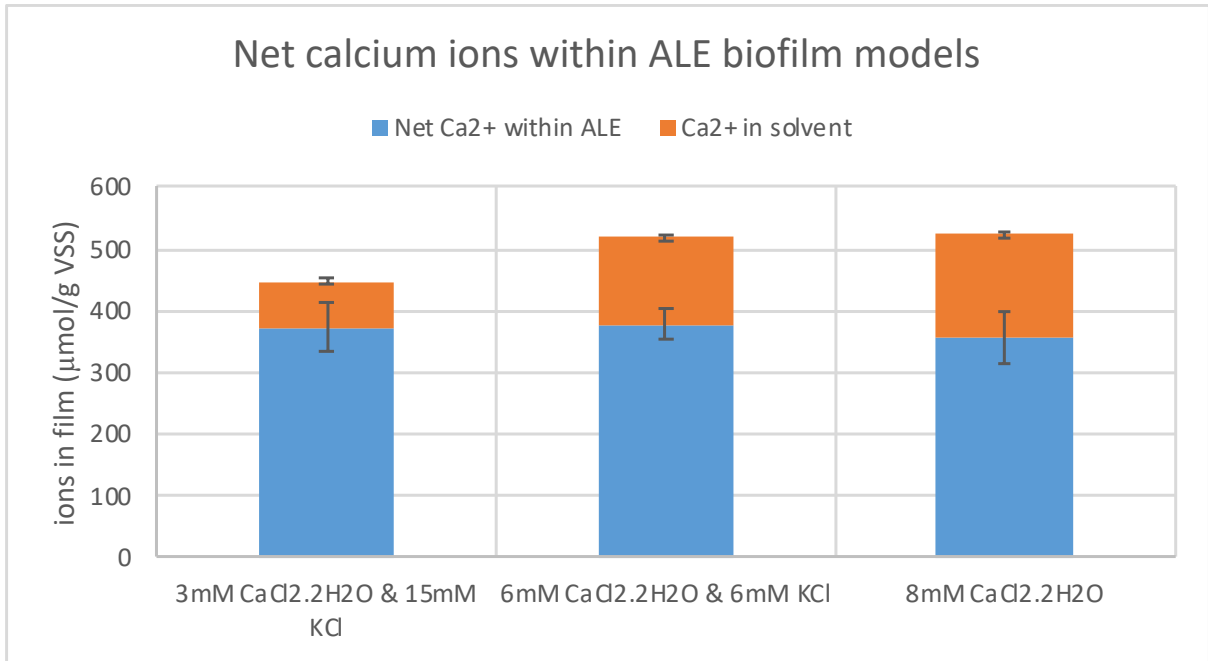


Figure 12 Net calcium ions within ALE biofilm models experiment series 1

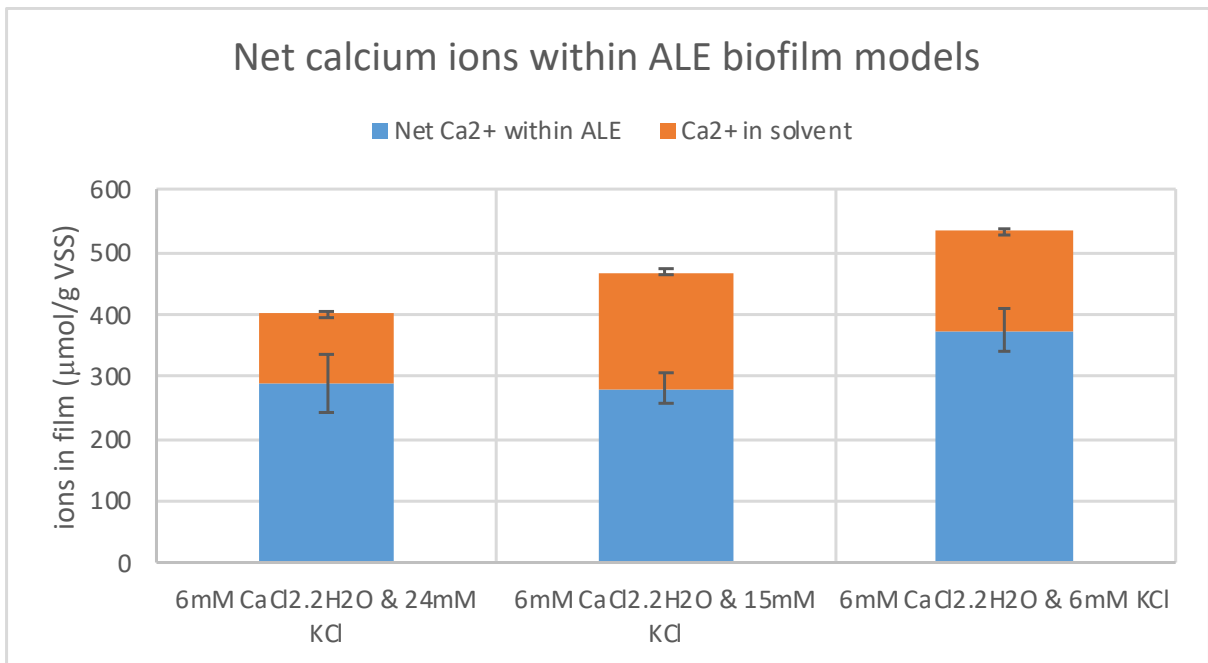


Figure 13 Net calcium ions within ALE biofilm models experiment series 2

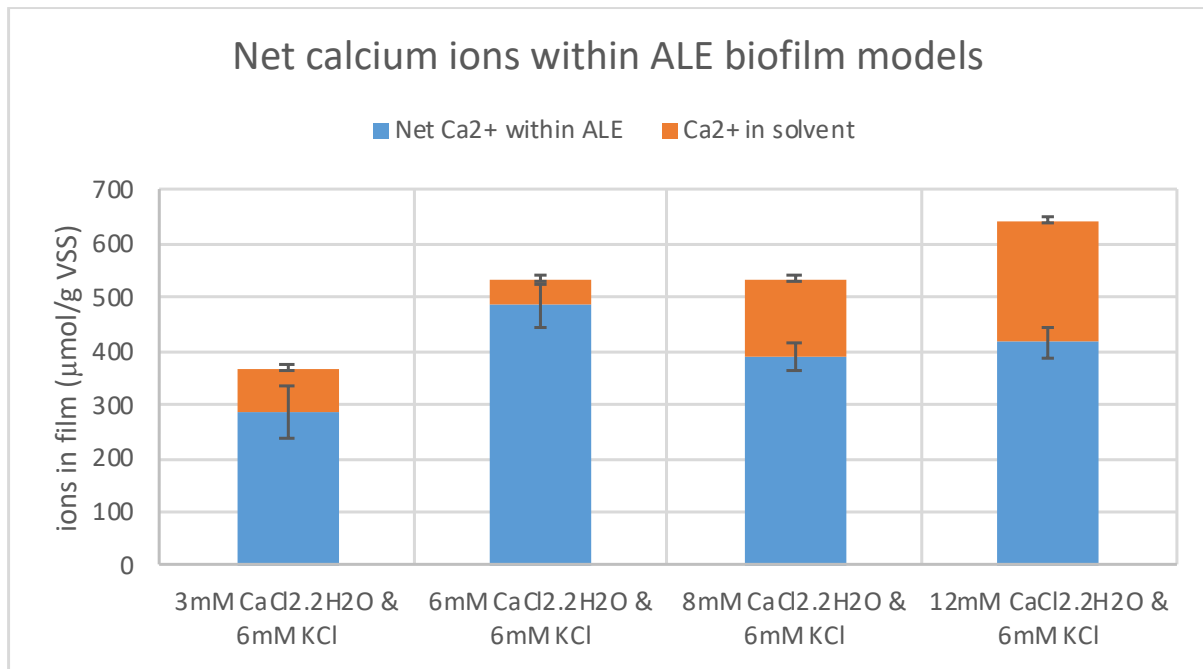


Figure 14 Net calcium ions within ALE biofilm models experiment series 3

As illustrated in Appendix 3, the majority composition of ALE biofilm models is organic which account for approximately 90% of total suspended solids. This amount is reasonable regarding the EPS property. However, the inorganic ash composition is not entirely from films themselves. Due to the intrinsic porosity of ALE biofilm models, they can absorb certain storage solution that has same ionic compositions as feed solution. The ion concentration of these inorganic ash was further investigated by IC and ICP-OES. The figures above present the number of calcium ions within the ALE biofilm models, where the absorbed ones were deducted. These calcium ions were assumed to build up the cake-layer of these films and thus contributed to their density. It is expected that higher calcium concentration in feed solution may contribute more calcium ions to ALE films. However, some error occurred probably caused by the deviation in IC and ICP-OES devices.

The effect of the ion concentration within the biofilm on its swelling behaviour

This part is the major research interest where time, swelling behaviour, and ALE biofilm models' inner ion concentrations are interrelated. To answer this research question, the relative swelling height against time was first plotted to demonstrate the net swelling behaviour for each sample. Afterwards, the VSS density over time was plotted to get an insight on the influence of dry mass composition on the ALE biofilm models. Finally, the relationship between the ion composition within the ALE biofilm and its swelling behaviour was illustrated. The samples with only KCl in feed solution were not included.

Experiment series one

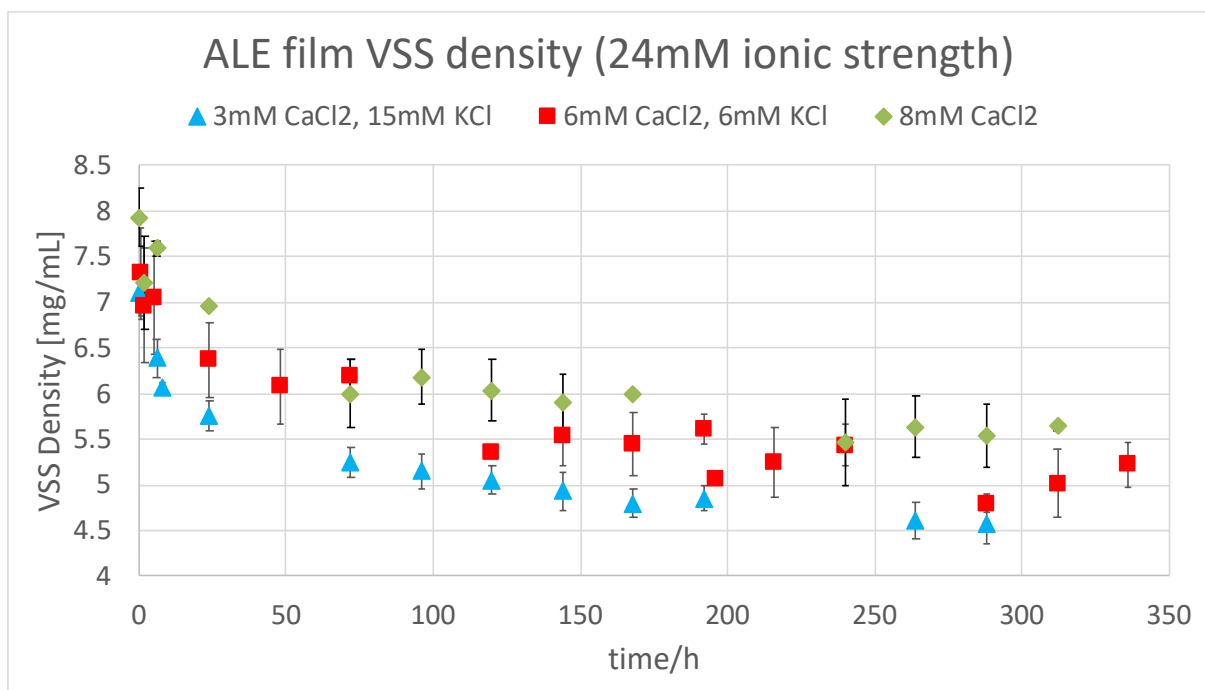
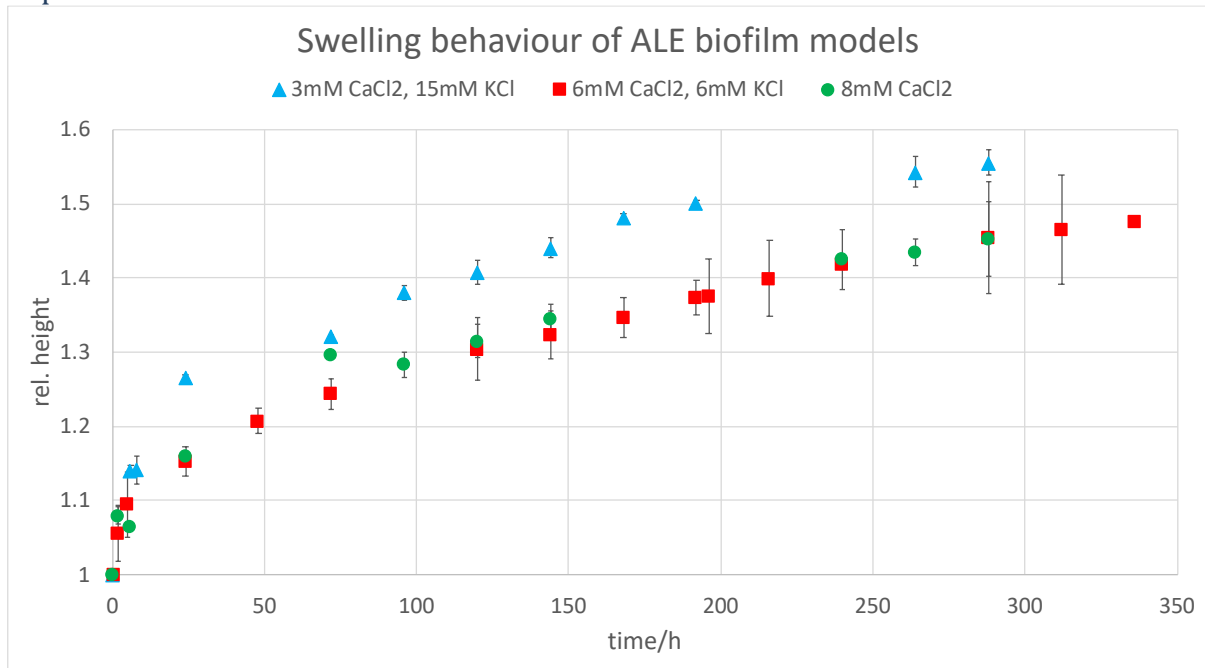


Figure 15 Swelling behaviour and VSS density overtime experiment series one

Experiment series two

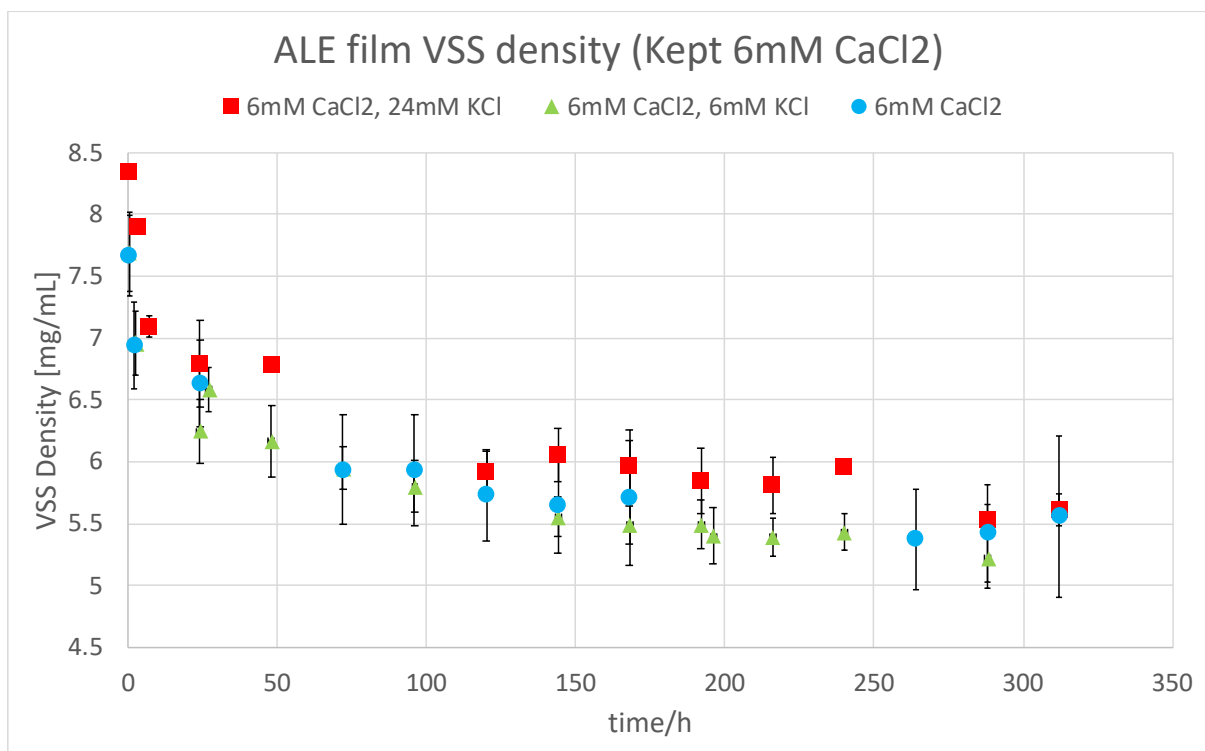
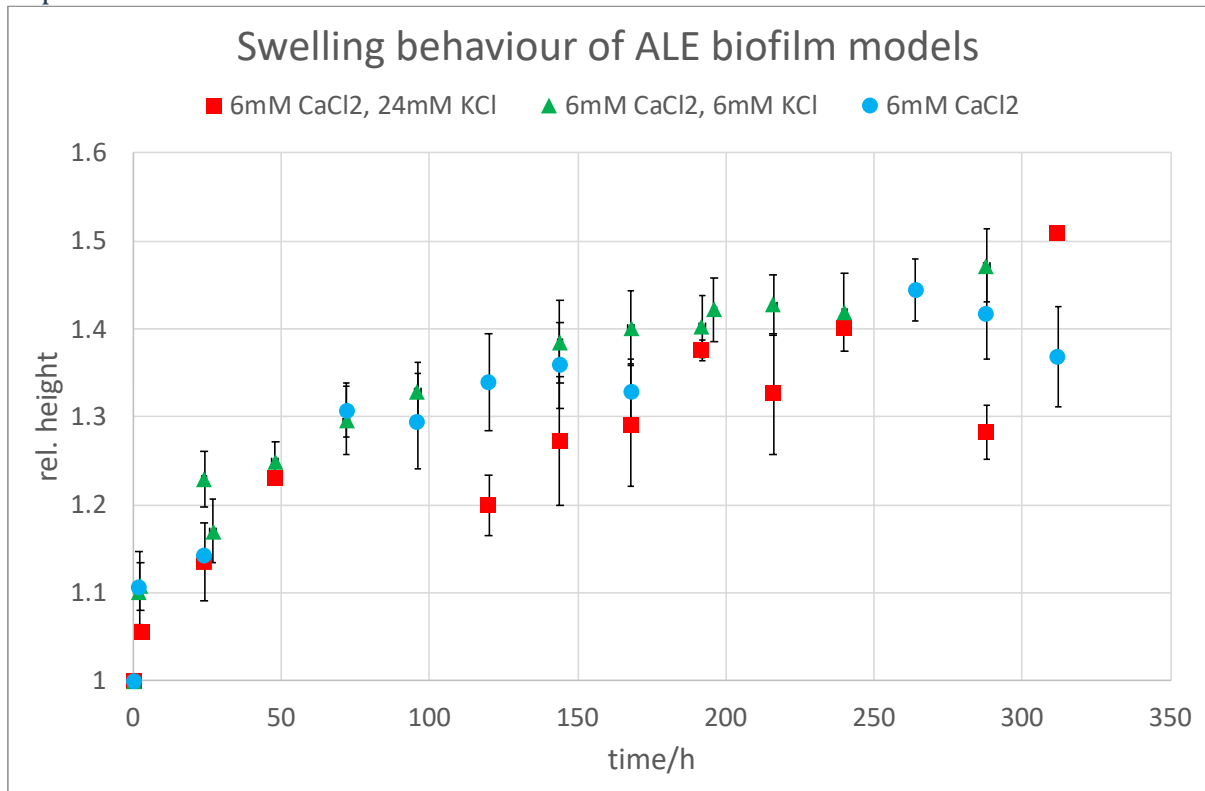


Figure 16 Swelling behaviour and VSS density overtime experiment series two

Experiment series three

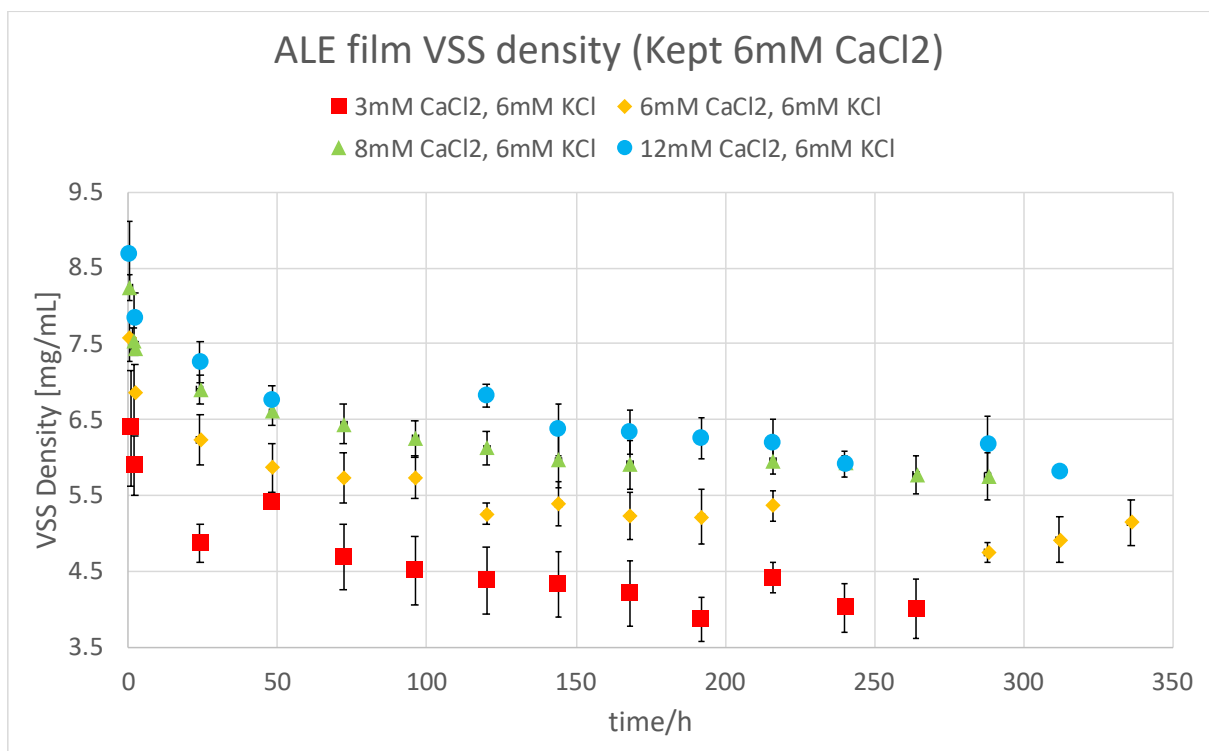
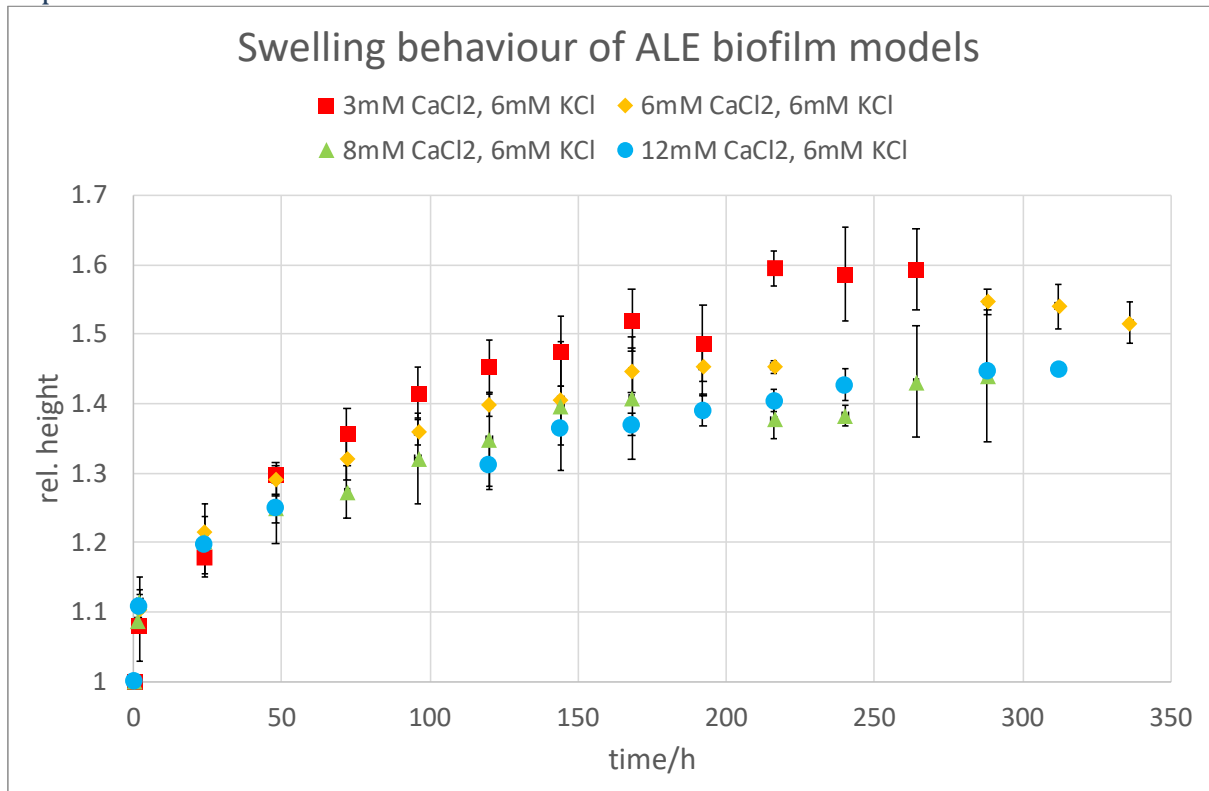


Figure 17 Swelling behaviour and VSS density overtime experiment series three

The data retrieved from first 200 hours distributed steadier than rest ones. From experiment series one and three, where calcium ion in feed solution is controlled at 3mM the ALE biofilm models experienced the most swelling. As illustrated, 3mM CaCl₂ is the threshold on the ALE biofilm models swelling behaviour. Above 3mM calcium ions, higher calcium concentration does not have much influence on their swelling, while more calcium ions contribute to the density namely the strength of the films. The KCl concentration did not contribute much to the swelling behaviour and did not have conclusive influence to the films' density. As one of the major interests in density, the resistance of ALE biofilm models will be discussed in the following chapter.

The variation of cake-layer resistance

As one of the major parameters in density, cake-layer resistance is strongly related to biofilm structural integrity which hampers the membrane filtration efficiency. Understanding cake-layer resistance within the biofilm is the first step to design tailored cleaning strategy. This project indicates that the changing ion concentration within the feed solution can influence the cake-layer resistance of ALE biofilm models. Ionic strength may also play an important role in defining cake-layer resistance.

Table 3 Time to reach the equilibrium state and Cake-layer resistance under different feed solutions

Order	Ionic strength	Feed solution concentration	Cake-layer resistance (m ⁻¹)
1	6mM	6mM KCl	9,595*10 ¹²
2	15mM	3mM CaCl ₂ •2H ₂ O & 6mM KCl	1,540*10 ¹³
3	18mM	6mM CaCl ₂ •2H ₂ O	2,235*10 ¹³
4	24mM	24mM KCl	1,019*10 ¹³
5	24mM	3mM CaCl ₂ •2H ₂ O & 15mM KCl	1,685*10 ¹³
6	24mM	6mM CaCl ₂ •2H ₂ O & 6mM KCl	1,692*10 ¹³
7	24mM	8mM CaCl ₂ •2H ₂ O	1,200*10 ¹³
8	30mM	8mM CaCl ₂ •2H ₂ O & 6mM KCl	2,570*10 ¹³
9	33mM	6mM CaCl ₂ •2H ₂ O & 15mM KCl	1,705*10 ¹³
10	42mM	6mM CaCl ₂ •2H ₂ O & 24mM KCl	1,365*10 ¹³
11	42mM	12mM CaCl ₂ •2H ₂ O & 6mM KCl	3,300*10 ¹³

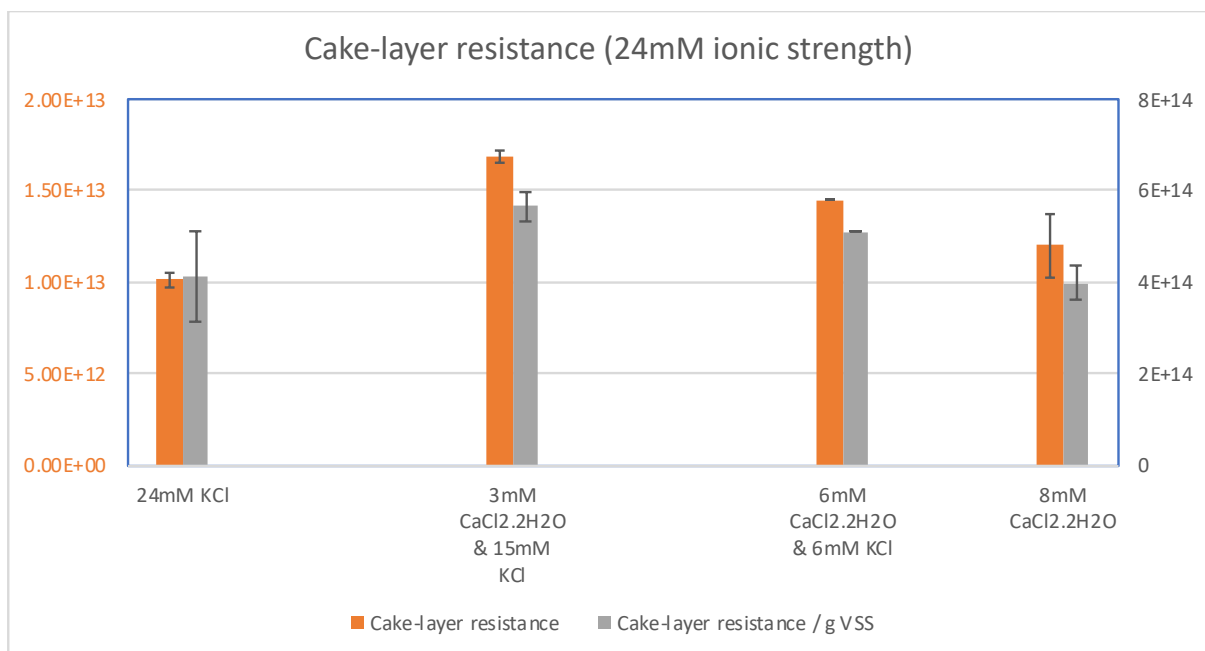
This table is composite by the ionic strength order. The value of cake-layer resistance in this table are taken the average of two samples. From order 2,6,8,11 in the table above, where KCl concentration is the same, the cake-layer resistance increases with the increased

concentration of $\text{CaCl}_2 \cdot 2\text{H}_2\text{O}$. Based on order 1,4 & 2,5 & 6,9, increased concentration of KCl also contributes the cake-layer resistance numerically. However, increased potassium ion composition in feed solution does not always increase the cake-layer resistance performance.



Figure 18 ALE biofilm models with only 6mM KCl in feed solutions. From left to right: 2 minutes after being taken out of Amicon cell; 20 minutes out of Amicon cell; 24 hours out of Amicon cell and be transported for the test.

The biofilm models with only KCl in feed solution are difficult to monitor their equilibrium state (see Figure 18). Although they contain a certain amount of cake-layer resistance numerically, ALE biofilms are easily detached from the base membrane and subsequently effortlessly disassembled under the minor external force during transportation.



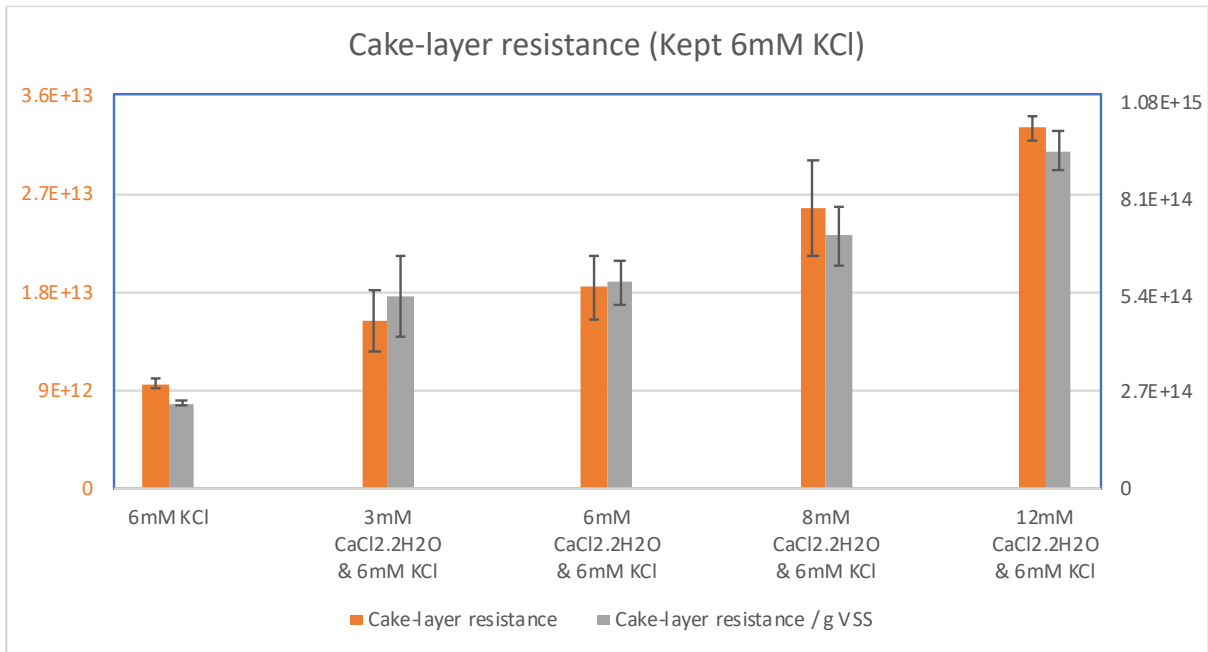
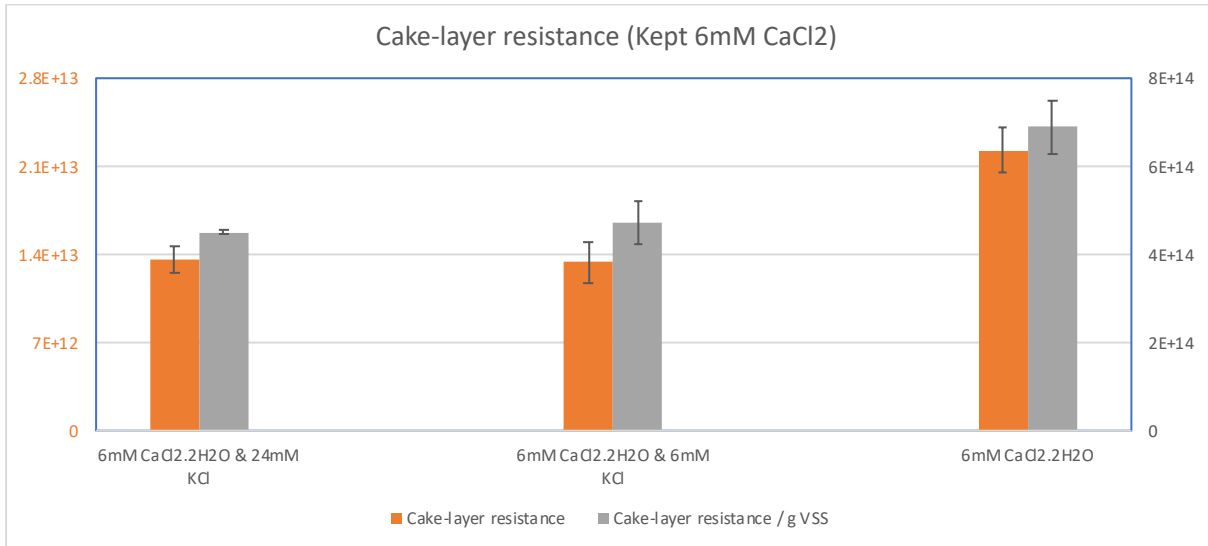


Figure 19 Normalised cake-layer resistance against VSS mass for each experiment series

From first two experiment series data, how dry mass compositions within the ALE biofilm models contribute to their resistance and density is not quite conclusive. The first experiment series suggests that increased KCl concentration contributes to the resistance, while the second experiment series seems to be random. However, in experiment series three, when KCl concentration was kept constant, the cake-layer resistance increases along with the increased concentration of calcium ions within feed solutions. This trend is in accordance with the density.

5. Discussion

This research is aiming to use the density of biofilm models made from alginate-like exopolymers (ALE) to profile their strength at their equilibrium swelling states. The models were produced under laboratory condition to control influencing factors. By comparing different compositions within models and identifying the vital components that contribute to biofilms' strength, weak points of biofilms can be identified to develop tailored cleaning strategies. However, some of the observed results were not conclusive and some of the phenomena were out of expectation.

General reflection: potential influence of microorganism

During OCT monitoring period, the internal porosity of ALE biofilm models existed certain days after production (see Figure 20). This phenomenon occurred for each monitored sample. This might be the swelling behaviour exceeded the texturing capacity of the film itself or the film had developed to a mature state that the biofilm tended to disperse for further colonization (see Figure 2, stage 5). If the porosity caused by the first assumption, a new method is needed for further investigation. If this caused by the microorganism, it is suggested to pre-treat the extracted ALE sludge samples, such as adding biocide in feed solution before ALE films production or freeze-dry the ALE sludge samples (currently all extracted ALE samples stored in -80°C condition).

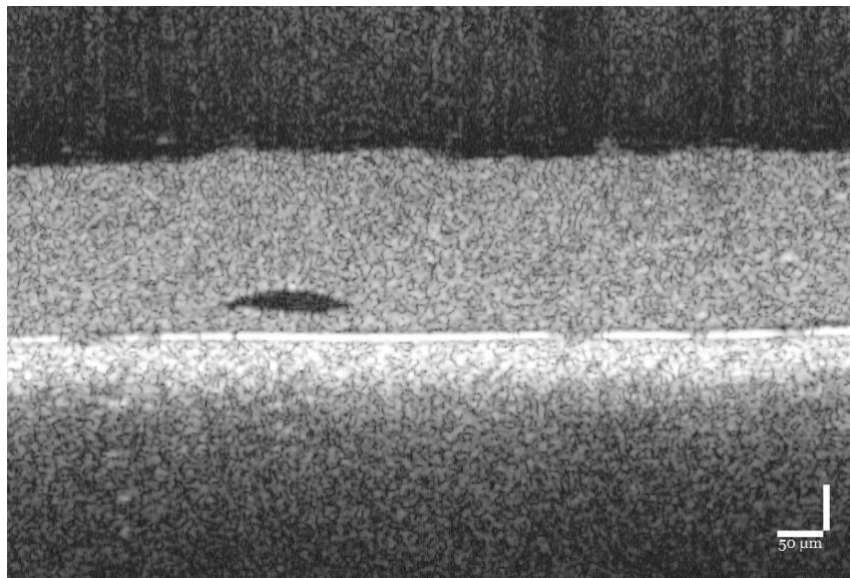


Figure 20 Internal porosity of one sample in experiment series 3, 3mM $\text{CaCl}_2 \cdot 2\text{H}_2\text{O}$ & 6mM KCl after 144hours

A structural hamper: the effect of transmembrane pressure

The biofilm models with only KCl in feed solution contain certain resistance values. However, according to equation (2) the total resistance of biofilm is directly proportional to the transmembrane pressure (TMP). The calculated cake-layer resistance is based on the pressure within the dead-end filtration cell. The pressure is set to 1 bar but usually drop to around 0.88 bar due to systemic loss. Therefore, all ALE films experienced a larger changing TMP when been taken out of the dead-end filtration system than expectation, which might cause the detachment of the KCl only samples. It is suggested to calibrate the Amicon cells presented in the filtration system regularly. Anyway, the performance of these samples proved the importance of calcium ions to biofilms structural integrity.

Other stochastic disturbances

The second experiment series does not show conclusive trend concerning the influence of KCl concentration. Various disturbances may cause this, for example, ALE biofouling accumulated within the dead-end filtration system; sample loss caused by air current during TSS/VSS sample transportation; deviation in IC and ICP-OES devices; time interference such as weekends and national holidays.

To mitigate the future fouling influence within the system, it is suggested to weekly clean the dead-end filtration system with 1 L, 2% NaClO solution to eliminate the microorganisms then rinse the system with at least 1 L, 1 mole NaOH solution to dissolve remained ALE biofouling. Rinsing the entire dead-end filtration system, especially the pipes and Amicon cells with excessive demi water afterwards to maintain moderate pH condition.

6. Conclusion & recommendation

This chapter will answer the research questions. Based on the indications in results and discussion chapter, proper recommendation for designing tailored biofouling cleaning strategies will be announced.

Answers to the research questions

Overall speaking, the calcium ions concentration is the vital element to the density of ALE biofilms rather than changing ionic strength and the presence of monovalent potassium ions.

RQ: What are the equilibrium states for the ALE biofilm models under different feed solutions?

According to Figure 15 to 17, the swelling data in first 200 hours distributed steadier than the others. This indicates that for ALE biofilm models produced with 120mg/L ALE in feed solution at 22°C and 1 bar pressure can reach their maximum steady swelling height, namely the equilibrium states around 200 hours.

RQ: How does different ionic composition within the feed solution affect the organic and inorganic content within an ALE biofilm model?

The feed solution with the concentration of 3mM CaCl₂ acts as the threshold to the ALE biofilm models' contents. Films produced at this concentration contains more water than the others. Therefore, these films have a lower density. The VSS density plots also prove this trend.

RQ: What effect has the ion composition within an ALE biofilm model on its swelling behaviour?

As illustrated in the swelling behaviour and VSS density charts, KCl concentrations alone has hardly any effect on the swelling behaviour, neither has the ionic strength according to the trends. Therefore, the difference in swelling behaviour observed are probably caused by the calcium concentration rather than by ionic strength or KCl concentration.

RQ: How does the cake-layer resistance vary along with the changing biofilm feed solutions?

The VSS density and the cake-layer resistance of ALE biofilm models are strongly related to calcium ions concentration within the feed solution. The gel-formation property of ALE biofilm models with the existence of calcium ions can contribute to their density. Starting from 3mM calcium ions in the feed solution, the ALE films experienced the largest swelling rate and the cake-layer resistance increases along with the increased calcium ions concentration. However, the swelling behaviour decreased when continue to increase the calcium concentration.

Recommendations for future experiments

As concluded calcium ion is vital to the density of ALE biofilm models and 3mM concentration is the threshold, it is recommended to test ALE biofilm models produced with only ALE and calcium ions in their feed solutions.

Recommendations for tailored cleaning strategies

To handle biofouling problems in real condition, maintaining the calcium ion concentration is necessary. Considering about the gel formation property and the high resistance value with the existence of high calcium concentration, it is wise to keep calcium ions at a lower concentration, for example, 3mM when the films contain more water. If the strength of biofilm decreased, alter fluid shear force to apply physical cleaning is easier, such as backwashing etc.

Bibliography

- Al-Ahmad, M., Aleem, F. A., Mutiri, A., & A. Ubaisy. (2000). Biofouling in RO membrane systems Part 1" Fundamentals and control. *Desalination*, 173-179.
- Arnal, J. M., García-Fayos, B., & Sancho, M. (2011). Membrane Cleaning. In P. R. Ning, *Expanding Issues in Desalination*. Shanghai: InTech.
- Bogino, P. C., Oliva, M. d., Sorroche, F. G., & Giordano, W. (2013). The Role of Bacterial Biofilms and Surface Components in Plant-Bacterial Associations. *International Journal of Molecular Sciences*, 15838-15859.
- Charfi, A., Harmand, J., Amar, N. B., Grasmick, A., & Heran, M. (2014). Deposit membrane fouling: influence of specific cake layer resistance and tangential shear stresses. *Water Science & Technology*, 40-46.
- Davidovich-Pinhas, M., & Bianco-Peled, H. (2009). A quantitative analysis of alginate swelling. *Carbohydrate Polymers*, 1020-1027.
- Derlon, N., Grütter, A., Brandenberger, F., Sutter, A., Kuhlicke, U., Neu, T. R., & Morgenroth, E. (2016). The composition and compression of biofilms developed on ultrafiltration membranes determine hydraulic biofilm resistance. *Water Research*, 63-72.
- Desmond, P., Best, J. P., Morgenroth, E., & Derlon, N. (2018). Linking composition of extracellular polymeric substances (EPS) to the physical structure and hydraulic resistance of membrane biofilms. *Water Research*, 211-221.
- D'Abzac, P., Bordas, F., Van Hullebusch, E., Lens, P. N., & Guibaud, G. (2010). Extraction of extracellular polymeric substances (EPS) from anaerobic granular sludges: comparison of chemical and physical extraction protocols. *Appl Microbiol Biotechnol*, 1589-1599.
- Dreszer, C., Vrouwenvelder, J., Paulitsch-Fuchs, A., Zwijnenburg, A., Kruihof, J., & Flemming, H.-C. (2013). Hydraulic resistance of biofilms. *Journal of Membrane Science*, 436-447.
- Dutch Water Sector. (2013, October 15). News. Retrieved February 16, 2018, from Water board Noorderzijlvest commissioned second Dutch Nereda plant at wwtp Garmerwolde: <https://www.dutchwatersector.com/news-events/news/7960-water-board-noorderzijlvest-commissioned-second-dutch-nereda-plant-at-wwtp-garmerwolde.html>
- Felz, S., Al-Zuhairy, S., Aarstad, O. A., Loosdrecht, M. C., & Lin, Y. M. (2016). Extraction of Structural Extracellular Polymeric Substances from Aerobic Granular Sludge. *Journal of Visualized Experiments*, 115/2-3.
- Flemming, H.-C., & Wingender, J. (2010). The biofilm matrix. *Nature Reviews Microbiology*, 623-633.

- Garrett, T. R., Bhakoo, M., & Zhang, Z. (2008). Bacterial adhesion and biofilms on surfaces. *Progress in Natural Science*, 1049-1056.
- Gerritse, J., & Huurne, P. t. (2011). *Biofouling potential reduction of waste water treatment effluents through biofiltration with Denutritor*. Deltares.
- Hou, X., & Jones, B. T. (2000). Inductively Coupled Plasma/Optical Emission Spectrometry. In R. Meyers, *Encyclopedia of Analytical Chemistry* (pp. 9468-9485). Chichester: John Wiley & Sons Ltd.
- Iorhemen, O. T., Hamza, R. A., & Tay, J. H. (2016). Membrane Bioreactor (MBR) Technology for Wastewater Treatment and Reclamation: Membrane Fouling. *Membranes*.
- Jiang, H.-L., Tay, J.-H., Liu, Y., & Tay, S. T.-L. (2002). Ca²⁺ augmentation for enhancement of aerobically grown microbial granules in sludge blanket reactors. *Biotechnology Letters*, 95-99.
- Kaplan, J. (2010). Biofilm Dispersal: Mechanisms, Clinical Implications, and Potential Therapeutic Uses. *Journal of Dental Research*, 205-218.
- Kersaan-Haan, M., & Heegstra, M. (2010). *Determination of elements in (waste) water by means of ICP-OES*. Leeuwarden: Wetsus.
- Lin, H., Zhang, M., Wang, F., Meng, F., Liao, B.-Q., Hong, H., . . . Gao, W. (2014). A critical review of extracellular polymeric substances (EPSs) in membrane bioreactors: Characteristics, roles in membrane fouling and control strategies. *Journal of Membrane Science*, 110-125.
- Lin, Y., de Kreuk, M., van Loosdrecht, M., & Adin, A. (2010). Characterization of alginate-like exopolysaccharides isolated from aerobic granular sludge in pilot-plant. *Water Research*, 3355-3364.
- Lin, Y., Sharma, P., & Loosdrecht, M. v. (2012). The chemical and mechanical differences between alginate-like exopolysaccharides isolated from aerobic flocculent sludge and aerobic granular sludge. *Water Research*, 57-65.
- Lyme, B. A. (2015, November 30). *Straight talk about biofilms: A new answer for treating Lyme disease?* Retrieved from Bay Area Lyme Foundation: <https://www.bayarealyme.org/blog/straight-talk-biofilms-new-answer-treating-lyme-disease/>
- McSwain, B. S., Irvine, R. L., Hausner, M., & Wilderer, P. A. (2005). Composition and Distribution of Extracellular Polymeric Substances in Aerobic Flocs and Granular Sludge. *Applied and Environmental Microbiology*, 1051-1057.
- Melo, L. F., Bott, T. R., Fletcher, M., & Capdeville, B. (1992). *Biofilms – Science and Technology*. Dordrecht: Springer-Science+Business Media.

- Microdyn NADIR. (2018, February 9). *The Art to Clear Solutions*. Retrieved February 15, 2018, from NADIR® Membranes: <http://www.microdyn-nadir.com/en/products/nadir/>
- Nguyen, T., Roddick, F. A., & Fan, L. (2012, November 21). Biofouling of Water Treatment Membranes: A Review of the Underlying Causes, Monitoring Techniques and Control Measures. *Membranes (Basel)*, 804-840.
- Nicolaisen, B. (2002, April 12). *Water and Wastes Digest*. Retrieved December 31, 2017, from Membranes: fouling & cleaning: <https://www.wwdmag.com/membranes-microfiltration/membranes-fouling-cleaning>
- Pronk, M., Neu, T., Loosdrecht, M. v., & Lin, Y. (2017). The acid soluble extracellular polymeric substance of aerobic granular sludge dominated by *Deffluviococcus* sp. *Water Research*, 148-158.
- Royal HaskoningDHV. (2013). *Nereda*. Retrieved February 16, 2018, from The Netherlands-Garmerwolde: <https://www.royalhaskoningdhv.com/en-gb/nereda/nereda-wastewater-treatment-plants/the-netherlands-garmerwolde/490>
- Salsabil, M., Laurent, J., Casellas, M., & Dagot, C. (2010). Techno-economic evaluation of thermal treatment, ozonation and sonication for the reduction of wastewater biomass volume before aerobic or anaerobic digestion. *Journal of Hazardous Materials*, 323-333.
- Seviour, T., Yuan, Z., van Loosdrecht, M. C., & Lin, Y. (2012). Aerobic sludge granulation: A tale of two polysaccharides? *Water Research*, 4803-4813.
- Sinniah, K., & Piers, K. (2001). Ion Chromatography: Analysis of Ions in Pond Waters. *Journal of Chemical Education*, 358-362.
- Stoodley, P., Sauer, K., Davies, D., & Costerton, J. (2002). Biofilms as complex differentiated communities. *Annual Review of Microbiology*, 187-209.
- Strathmann, M., Griebe, T., & Flemming, H.-C. (2000). Artificial biofilm model - A useful tool for biofilm research. *Applied Microbiology and Biotechnology*, 231-237.
- van der Borden, A. J., van der Werf, H., van der Mei, H. C., & Busscher, H. J. (2004). Electric Current-Induced Detachment of *Staphylococcus epidermidis* Biofilms from Surgical Stainless Steel. *Applied and Environmental Microbiology*, 6871-6874.
- Wartena, P. (2010). *Determination of anions using ion chromatograph*. Leeuwarden: Wetsus.
- Williams, P. A. (2007). *Handbook of Industrial Water Soluble Polymers*. Blackwell Publishing Ltd.
- Wingender, J., Neu, T. R., & Flemming, H.-C. (1999). *Microbial Extracellular Polymeric Substances: Characterization, Structure and Function*. Heidelberg: Springer.

Appendix 1: Functions of EPS in bacterial biofilms

Table 1 Functions of extracellular polymeric substances in bacterial biofilms (Flemming & Wingender, 2010)

Function	Relevance for biofilms	EPS components involved
Adhesion	Allows the initial steps in the colonization of abiotic and biotic surfaces by planktonic cells, and the long-term attachment of whole biofilms to surfaces	Polysaccharides, proteins, DNA and amphiphilic molecules
Aggregation of bacterial cells	Enables bridging between cells, the temporary immobilization of bacterial populations, the development of high cell densities and cell-cell recognition	Polysaccharides, proteins and DNA
Cohesion of biofilms	Forms a hydrated polymer network (the biofilm matrix), mediating the mechanical stability of biofilms (often in conjunction with multivalent cations) and, through the EPS structure (capsule, slime or sheath), determining biofilm architecture, as well as allowing cell-cell communication	Neutral and charged polysaccharides, proteins (such as amyloids and lectins), and DNA
Retention of water	Maintains a highly hydrated microenvironment around biofilm organisms, leading to their tolerance of desiccation in water-deficient environments	Hydrophilic polysaccharides and, possibly, proteins
Protective barrier	Confers resistance to nonspecific and specific host defences during infection, and confers tolerance to various antimicrobial agents (for example, disinfectants and antibiotics), as well as protecting cyanobacterial nitrogenase from the harmful effects of oxygen and protecting against some grazing protozoa	Polysaccharides and proteins
Sorption of organic compounds	Allows the accumulation of nutrients from the environment and the sorption of xenobiotics (thus contributing to environmental detoxification)	Charged or hydrophobic polysaccharides and proteins
Sorption of inorganic ions	Promotes polysaccharide gel formation, ion exchange, mineral formation and the accumulation of toxic metal ions (thus contributing to environmental detoxification)	Charged polysaccharides and proteins, including inorganic substituents such as phosphate and sulphate
Enzymatic activity	Enables the digestion of exogenous macromolecules for nutrient acquisition and the degradation of structural EPS, allowing the release of cells from biofilms	Proteins
Nutrient source	Provides a source of carbon-, nitrogen- and phosphorus-containing compounds for utilization by the biofilm community	Potentially all EPS components
Exchange of genetic information	Facilitates horizontal gene transfer between biofilm cells	DNA
Electron donor or acceptor	Permits redox activity in the biofilm matrix	Proteins (for example, those forming pili and nanowires) and, possibly, humic substances
Export of cell components	Releases cellular material as a result of metabolic turnover	Membrane vesicles containing nucleic acids, enzymes, lipopolysaccharides and phospholipids
Sink for excess energy	Stores excess carbon under unbalanced carbon to nitrogen ratios	Polysaccharides
Binding of enzymes	Results in the accumulation, retention and stabilization of enzymes through their interaction with polysaccharides	Polysaccharides and enzymes

Appendix 2: Detailed experiment protocols

- Sonication EPS extraction
 - Transfer 5 g (wet weight) of granules in a 250 ml baffled flask and fill up the flask to 50 ml with demineralized water.
 - Put the flask containing the mixture into a 1000 ml glass beaker that half-filled with ice.
 - Apply pulsed sonication on ice for 3 min at 50 W to the mixture (Felz, Al-Zuhairy, Aarstad, Loosdrecht, & Lin, 2016).

- High temperature - sodium carbonate EPS extraction
 - Pre-heat 150 ml tap water in a 1000 ml glass beaker on a magnetic stirrer to 80 °C.
 - Add 0.25 g Na₂CO₃ anhydrous or 0.67 g Na₂CO₃•10H₂O into the flask to obtain a 0.5% (w/v) Na₂CO₃ concentration.
 - Put the flask containing the mixture into the water bath. Cover the flask and the beaker glass separately with aluminium foil to prevent evaporation.
 - Stir the mixture for 35 min at 400 rpm and 80 °C.
 - Transfer the mixture to a 50 ml centrifugation tube.
 - Centrifuge the centrifugation tube containing the mixture at 4,000 × g and 4 °C for 20 min.
 - Collect the supernatant and discard the pellet (Felz, Al-Zuhairy, Aarstad, Loosdrecht, & Lin, 2016).

- Alginate-like Exopolysaccharides (ALE) Extraction
 - Transfer the dialyzed extract into a 250 ml glass beaker. Slowly stir the extraction at 100 rpm and room temperature. Constantly monitor pH changes with a pH electrode, while adding 1 M hydrochloric acid (HCl) to a final pH of 2.2 ± 0.05 to obtain ALE in the acidic form.
 - After adjusting the pH to 2.2, transfer the extract into a 50 ml centrifugation tube and centrifuge at 4,000 × g and 4 °C for 20 min.
 - Discard the supernatant and collect the gel-like pellet. The gel-like pellet is ALE in the acidic form.
 - To obtain the sodium (or potassium) form of ALE, slowly add 0.5 M NaOH (or 0.5 M potassium hydroxide) to the gel obtained above, while mixing the gel slowly with a glass stick by hand until pH 8.5 is reached. (Felz, Al-Zuhairy, Aarstad, Loosdrecht, & Lin, 2016) Extra ALE samples are stored in -80 °C condition.

- Ionic Hydrogel Formation Test
 - Take the extracted sodium ALE and slowly drip small portion of the extract with a Pasteur pipette into a 2.5% (w/v) calcium chloride (CaCl₂) solution.

- Preparation of 2L feed solution
 - To understand the influence of cations' concentration to the strength and the swelling behaviour of ALE biofouling, a series of different concentrations of ALE feed solutions will be needed.

- First, dissolve ALE in $\pm 0.5L$ (1h stirring), then add salts in $\pm 1L$, fill up to 2L (stir again 1h)
- Amicon cell filtration runs until approx. 0.6 L is filtered (takes around 16hours)
 - First clean-water flux, 1L (about 20min) for both
 - When finished store in the salt solution of the same concentration as feed (without ALE)
- OCT
 - Pictures and height
 - Immediately (usually 10-30min after stopping the cells)
 - 2h
 - 20-24h
 - 2 days
 - 3 days
 - 5 days
 - 9 days
- Analyses
 - TSS/VSS
 - 24h at 105 °C \rightarrow water evaporates \rightarrow total suspended solids (TSS)
 - 2h at 550 °C \rightarrow organics are oxidised \rightarrow remains are only the inorganic compounds (missing weight = volatile suspended solids, VSS)
 - Further analysis of ash to determine calcium content
 - ICP-OES
 - Microwave digestion in 69% HNO₃, then diluted 35 times and hand in for ICP-OES, asking for Calcium, Potassium, Sodium, Iron, Sulphur, and Boron
- Interpretation
 - Graph and Table including
 - Feed composition
 - Actual composition (VSS, water, Ca/K/Na)
 - Initial height (+ VSS and Ca density)
 - Equilibrium height (+ VSS and Ca density)
 - Days until equilibrium

Appendix 3: TSS/VSS percentage plots R coding

```
library(ggplot2)
library(ggthemes)
library(extrafont)
library(plyr)
library(scales)
charts.data <- read.csv("tss.csv")

#Basic graph
tss <- ggplot() + geom_bar(aes(y = percentage, x = feed, fill = part), data = charts.data,
                          stat="identity")
tss

#Adjusting data labels position
charts.data <- ddply(charts.data, .(feed),
                    transform, pos = cumsum(percentage) - (0.5 * percentage))

tss <- ggplot() + geom_bar(aes(y = percentage, x = feed, fill = part), data = charts.data,
                          stat="identity")
tss <- tss + geom_text(data=charts.data, aes(x = feed, y = pos, label = paste0(percentage,"%")),
                      size=4)
tss

#Adjusting legend position
tss <- tss + theme(legend.position="bottom", legend.direction="horizontal",
                  legend.title = element_blank())
tss

#Adjusting axis, title & units
tss <- tss + labs(x="Feed Solution", y="Percentage") +
  scale_y_continuous(labels = dollar_format(suffix = "%", prefix = "")) +
  ggtitle("Average TSS percentage (%)")
tss

#Adjusting color palette
fill <- c("#b58446", "#86c1f4")
tss <- tss + scale_fill_manual(values=fill)
tss
```

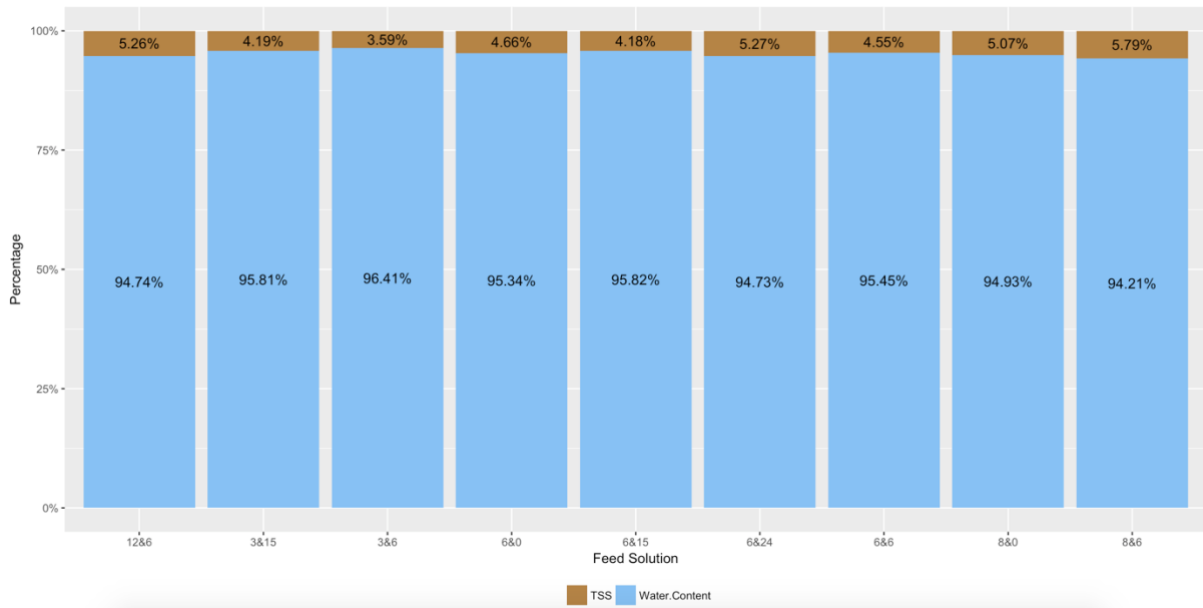


Figure 1 Average TSS percentage VS different feed solutions

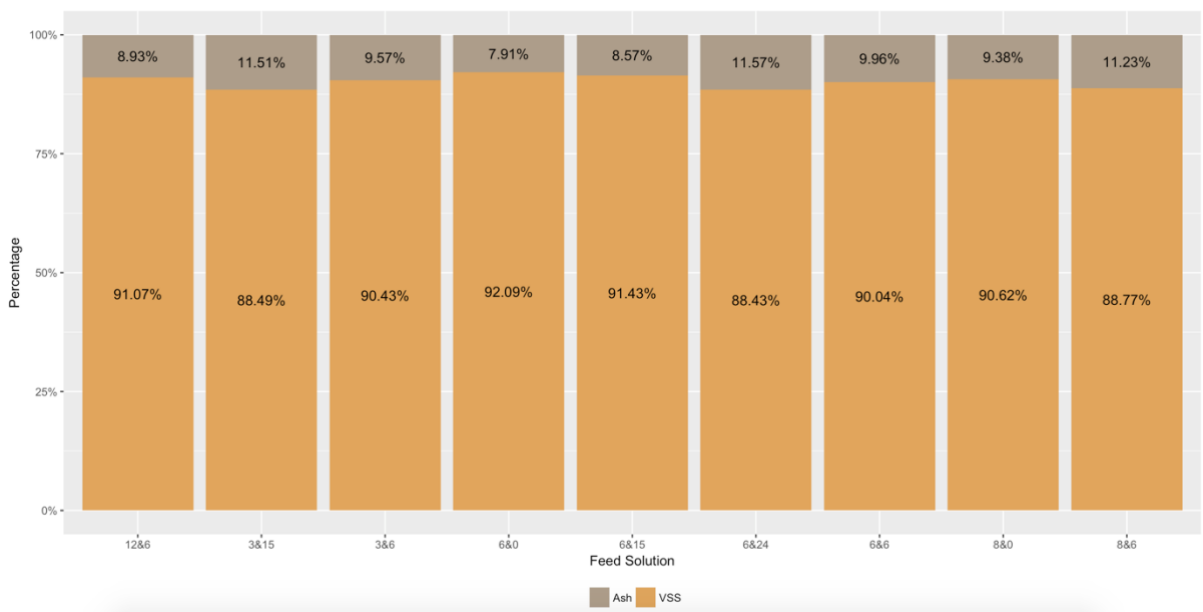


Figure 2 Average VSS percentage VS different feed solutions